



Differential impact of dose-range glyphosate on locomotor behavior, neuronal activity, glio-cerebrovascular structures, and transcript regulations in zebrafish larvae

Isabel Forner-Piquer, Adèle Faucherre, Julia Byram, Marine Blaqui re, Fr d ric de Bock, Laurence Gamet-Payrastre, Sandrine Ellero-Simatos, Etienne Audinat, Chris Jopling, Nicola Marchi

► To cite this version:

Isabel Forner-Piquer, Ad le Faucherre, Julia Byram, Marine Blaqui re, Fr d ric de Bock, et al.. Differential impact of dose-range glyphosate on locomotor behavior, neuronal activity, glio-cerebrovascular structures, and transcript regulations in zebrafish larvae. *Chemosphere*, 2021, 267, pp.128986. 10.1016/j.chemosphere.2020.128986 . hal-03100578

HAL Id: hal-03100578

<https://hal.science/hal-03100578>

Submitted on 24 Sep 2021

HAL is a multi-disciplinary open access archive for the deposit and dissemination of scientific research documents, whether they are published or not. The documents may come from teaching and research institutions in France or abroad, or from public or private research centers.

L'archive ouverte pluridisciplinaire **HAL**, est destin e au d p t et   la diffusion de documents scientifiques de niveau recherche, publi s ou non,  manant des  tablissements d'enseignement et de recherche fran ais ou  trangers, des laboratoires publics ou priv s.

Differential impact of dose-range glyphosate on locomotor behavior, neuronal activity, glyo-cerebrovascular structures, and transcript regulation in zebrafish larvae.

Isabel Forner-Piquer¹, Adèle Faucherre³, Julia Byram¹, Marine Blaquiére¹, Frederic de Bock¹, Laurence Gamet-Payraastre², Sandrine Ellero-Simatos², Etienne Audinat¹, Chris Jopling³ and Nicola Marchi¹

¹ Cerebrovascular and Glia Research, Institute for Functional Genomics (University of Montpellier - UMR 5203 CNRS - U 1191 INSERM), 141 rue de la Cardonille, 34094 Montpellier (France)

²Toxalim, Research Centre in Food Toxicology (Université de Toulouse, INRAE, ENVT, INP-Purpan, UPS), 180 Chemin de tournefeuille, 31300 Toulouse (France)

³ Molecular mechanisms of regeneration, Institute for Functional Genomics (University of Montpellier - UMR 5203 CNRS - U 1191 INSERM LabEx ICST), 141 rue de la Cardonille, 34094 Montpellier (France)

Number of pages: 43
Words main text: 7146
Figures: 7
Tables: 3
Supplemental Text: Extended Method Sections
Supplemental Figures: 3
Supplemental Tables: 9
Supplemental movies: 4

Running Title: Glyphosate and the zebrafish larvae brain.

Keywords: glyphosate, zebrafish, neurovascular, microglia, behavior, electrophysiology.

Corresponding Authors: Dr. Nicola Marchi, Cerebrovascular and Glia Research, Institut de Génomique Fonctionnelle (CNRS UMR5203, INSERM U1191, University of Montpellier), 141 rue de la Cardonille, 34094 Montpellier, Cedex 5, France. Email nicola.marchi@igf.cnrs.fr.

Dr. Chris Jopling, Cardiac Development, Disease and Regeneration, Institut de Génomique Fonctionnelle (CNRS UMR5203, INSERM U1191, University of Montpellier), 141 rue de la Cardonille, 34094 Montpellier, Cedex 5, France. Email chris.jopling@igf.cnrs.fr

Acknowledgements: This work was supported by MUSE-Pestifish (Montpellier Université d'Excellence) with the complementary aid of ANSES-Epidimicmac, ANR-Hepatobrain, Association France Parkinson and the Fédération pour la Recherche sur le Cerveau. Work in the C.J lab is supported by a grant from the Fondation Leducq and Fondation pour la Recherche sur le Cerveau "Espoir en tête 2017". A.F was supported by a Fondation *Lefoulon-Delalande* postdoctoral fellowship with previous support provided by a Fondation pour la Recherche Médicale (FRM) postdoctoral fellowship. Supported by the LabexICST PhD program. A.F, and C.J are members of the Laboratory of Excellence « Ion Channel Science and Therapeutics » supported by a grant from the ANR. We would like to thank IPAM and the MGX platforms for technical assistance and data analyses (IGF, Montpellier, France). We would like to thank Dr. Julie Perroy (IGF) for discussion and insights.

Conflicts of interest: none

Abstract

The presence of glyphosate represents a debated ecotoxicological and health risk factor. Here, zebrafish larvae were exposed, from 1.5 to 120 hours post-fertilization, to a broad concentration range (0.05 to 10.000 µg/L) of glyphosate to explore its impact on the brain. We evaluated morphology, tracked locomotor behavior and neurophysiological parameters, examined neuro-glio-vascular structures, and outlined transcriptomic deregulations by RNA sequencing.

At the concentration range tested, glyphosate did not elicit gross morphological changes. Next, behavioral analysis revealed a significant decrease in locomotor activity following exposure to 1000 µg/L, or higher. In parallel, midbrain electrophysiological recordings indicated abnormal spike activity in zebrafish larvae exposed to 1000 µg/L. Subsequently, we asked whether the observed neurophysiological outcome could be secondary to brain structural modifications. To this end, we used transgenic zebrafish and *in vivo* 2-photon microscopy to examine the effects of the behavior-modifying concentration of 1000 µg/L, comparing to 0.1 µg/L and control. We ruled out the presence of cerebrovascular and neuronal malformations. However, we observed microglia morphological modifications at low and high glyphosate concentrations, including the presence of amoeboid cells suggestive of activation. Lastly, RNAseq analysis showed the deregulation of transcript families implicated in neuronal physiology, synaptic transmission or inflammation, as evaluated at the two selected glyphosate concentrations.

In zebrafish larvae, behavioral and neurophysiological defects occur only after exposure to high glyphosate concentrations while, at cellular and transcript levels, pathological elements can be detected in response to low doses. The prospective

103 applicability to ecotoxicology and a possible extension to health vulnerability are
104 discussed.

105

106

107

108

109

110

111

112

113

114

115

116

117

118

119

120

121

122

123

124

125 **Highlights**

126 1. In zebrafish larvae, behavioral and brain electrophysiological defects elicit at high
127 glyphosate concentrations.

2. Neurological outcomes are not associated with structural neuro-vascular or muscular malformations.

3. Morphological signs of microglia activation are reported after exposure to low and high glyphosate concentrations.

4. Transcriptomic analysis reveals the deregulation of candidate pathways, possibly extending to neuronal vulnerability.

Introduction

Accumulating epidemiological studies outline a link between exposure to pesticides and central nervous system (CNS) disorders (Hernández et al., 2016; Roberts et al., 2019; Von Ehrenstein et al., 2019). Here we focus on glyphosate, a commonly used herbicide that is raising environmental and health risk alarms (Benbrook, 2016; Landrigan and Belpoggi, 2018; Van Bruggen et al., 2018; Vandenberg et al., 2017). Although glyphosate was designed to target the plant shikimate pathway (Sealey et al., 2016), concerns are emerging due to its suspected and highly debated multi-organ toxicity in experimental models or humans (Myers et al., 2016; Van Bruggen et al., 2018; Vandenberg et al., 2017; Von Ehrenstein et al., 2019).

Currently, glyphosate can be detected in environmental and biological matrices, including water and human fluids (Myers et al., 2016; Niemann et al., 2015; Van Bruggen et al., 2018). Epidemiological studies have suggested a potential association between exposure to glyphosate and neurodevelopmental disorders, including autism (Garry et al., 2002; Ongono et al., 2020; Sealey et al., 2016; Von Ehrenstein et al., 2019). Experimentally, the neurotoxic effects of glyphosate were reported, although using high concentrations. These studies revealed that, in zebrafish, elevated levels of glyphosate can induce developmental delay and neuronal damage (Roy et al., 2016; Sandrini et al., 2013; Zhang et al., 2017). At present, assessing the risks associated with the exposure to low concentrations of glyphosate is necessary (Annett et al., 2014; Van Bruggen et al., 2018).

Here, we systematically exposed zebrafish larvae to a wide range of glyphosate concentrations (0.05 to 10.000 µg/L), taking into account international

guidelines that define varying thresholds (see Methods). We begin by exploring the effects elicited by ranging glyphosate on anatomy and behavior. Based on the results obtained, we next performed *in vivo* brain 2-photon microscopy and transcriptomic analyses specifically investigating the effects triggered by a high and a low glyphosate concentration. We report and discuss the varying, or lack thereof, effects that concentrations of glyphosate can exert on the zebrafish larvae brain.

MATERIALS AND METHODS

Zebrafish strains and husbandry.

Zebrafish (*Danio rerio*, wild type AB strain) were maintained under standardized conditions and experiments were conducted in accordance with local approval (APAFIS#4054-2016021116464098 v5) and the European Communities council directive 2010/63/EU. Embryos were staged as described (Kimmel et al., 1995). All larvae were euthanised by administration of excess anaesthetic, tricaine methane sulfonate (300 mg/L; MS222, Sigma-Aldrich). Three zebrafish transgenic lines expressing fluorescent proteins in specific brain cells types were used: Endothelium-*Tg(fli1a:GFP)y1Tg* was provided by the CMR[B] *Centro de Medicina Regenerativa de Barcelona*, Microglia-*Tg(mpeg1:mCherry)* was created as previously described (Bernut et al., 2014), and Neurons-*Tg(HuC:Tomato)* was generated inhouse.

Glyphosate exposure protocol and morphological assessments.

Glyphosate [N-(Phosphonomethyl) glycine, CAS Number 1071-83-6], was purchased from Sigma-Aldrich (France) at 98,5% purity. All experiments were performed using water-based E3 medium to obtain the working glyphosate concentrations. Zebrafish larvae were exposed to 8 concentrations of glyphosate: 0.05, 0.1, 0.5, 1, 10, 100, 1000, 10.000 µg/L in E3 medium from 1.5 to 120 hours post fertilization (hpf). Solutions were renewed every day. The range here studied is broad and it includes: i) glyphosate concentrations that are lower or equal to the European drinking and ground water limit (Council Directive 98/83/EC, and 2006/118/EC), setting a maximum concentration of 0.1 µg/L for an individual

pesticide. Environmentally relevant glyphosate concentrations are also listed in (Carles et al., 2019; Hanke et al., 2010; Scribner et al., 2007; Uren Webster et al., 2013); ii) the maximum contaminant level in the US (700 µg/L), the health based guideline value in Australia (1000 µg/L), and the maximum acceptable concentration for glyphosate in drinking water in Canada (280 µg/L) (Canada Health, 2019; Székács and Darvas, 2018); iii) mg/L ranges that can be occasionally reported in areas where the use of glyphosate is significant and due to accidental peak pollution (Székács and Darvas, 2018; Uren Webster et al., 2013). The Extended Method section provides information inherent to glyphosate water quantification and re-test in our experimental conditions and the protocol used for zebra fish larvae morphology assessment.

Locomotor behavioral activity parameters.

At 120 hpf, all larvae were transferred in a multi-well plate and acclimatized for 60 minutes in the incubator (28 °C, dark) prior to testing. The multi-well plate was re-positioned in the observation chamber for 3 minutes of further acclimation (28 °C, dark). Consistently with the OECD guidelines #236 (Fish Embryo Acute Toxicity Test, 2013) testing was conducted in duplicate (2 plates, n=24/plate) for each concentration. Locomotor activity was recorded in a dark environment in a DanioVision observation chamber coupled with Ethovision video tracking v.14 (Ethovision XT, Noldus Information Technology, Netherlands). Data were smoothed with a Minimal Distance Moved threshold of 0.2 mm and with a Maximum Distance Moved filter of 8 mm to exclude small movements. See extended Methods Section.

Phalloidin staining of actin fibers.

120 hpf zebrafish larvae obtained from CTRL, 0.1, 1000 and 10000 µg/L glyphosate conditions were fixed in a 4% PFA solution for 3 hours at room temperature and rinsed with PBS (duplicate, n=7/group). Larvae were permeabilized using PBS + triton 0.1%. Phalloidin working solution (1X) was prepared by adding 1 µL of Phalloidin-iFluor 594 (ab 176757) stock solution (-20 °C) into 1mL of PBS + 0.5% Bovine Serum Albumin (BSA). The phalloidin working solution was added for 2h in the dark. Next, larvae were washed in PBS and mounted on a drop of methylcellulose. Images (Z-stack, 20X) were taken using an Apotome Zeiss ImagerZ.1 and processed using Zen 3.2 software. The length of the fast-twitch fibers was assessed using ImageJ. Phalloidin was previously used to study muscle defects in (Han et al., 2020; Jia et al., 2020; Snow et al., 2008).

In vivo 2-photon neuro-glio-vascular analysis.

Tg(fli1a:GFP)y1Tg:Tg(mpeg1:mCherry) larvae from CTRL, 0.1 and 1000 µg/L glyphosate conditions (duplicate, n=5/group) were anesthetized using tricaine (1mL 25x 50mL E3 medium) and immobilized in a drop of low-melting point agarose. N-phenylthiourea (PTU) was added once a day to the E3 medium to prevent pigmentation, from 24 to 96 hpf, with a final concentration of 0.002 mL PTU/mL E3. *In vivo* whole head z-stack images were acquired at the IPAM platform (Imagerie du Petit Animal de Montpellier) using a 2-photon Olympus FV-MPE RS microscope coupled with Coherent Chameleon Vision II and Spectra Insight X3 lasers adapted to zebrafish imaging. 3D cerebrovascular maps were generated using IMARIS 9.1.2

(Oxford Instruments). We selected the midbrain as Region of interest (ROI), specifically the area between the metencephalic artery (MtA) and anterior cerebral vein (ACeV), following the annotations of the Interactive atlas of zebrafish anatomy (<https://zfish.nichd.nih.gov/FinalDesign1/DiagPage.html>). We quantified the following structures in the 3D domain: i) lengths or volumes of the cerebrovasculature, ii) microglia volume, and iii) microglia-vessel distributions. We selected a specific volume included within the mesencephalic veins (MsV) and the ACeV to classify microglial cells based on their morphology (soma size and process length), into 3 subtypes: ameboid/activated, rod-like, or resting (Perry et al., 2010). Using the *Tg(HuC:Tomato)* zebra fish line and the protocol described above images were acquired. Optic nerve length, thickness of the optic nerve, length of the optic tectum, and 1st hindbrain axon extensions were measured using ImageJ.

Zebrafish in vivo electrophysiology.

Electrophysiological field potential recordings were performed *in vivo* as previously described (Baraban, 2013) using 120 hpf zebrafish larvae (n=13 CTRL, n=13 0.1 µg/L glyphosate, n=21 1000 µg/L glyphosate). Animals were paralyzed using 300 µM of pancuronium (Abcam) diluted in E3 medium for 5 minutes and mounted in low-melting point agarose on a small glass culture dish. Next, the dish was placed under a macroscope Leica Z16 APO and a glass microelectrode was manually positioned in the midbrain region. The microelectrode was filled with PBS. Extracellular field potential activity was recorded for at least 1 hour using a custom-made amplifier (1000X, bandwidth 1hz-1khz) and digitized using Digidata 1440 (Molecular Devices). Data were analyzed using Clampfit v11.0.3 focusing on a 20-30

minutes period selected after the initial 10-15 minutes of recording, to avoid biases due to stabilization. Zebra fish preparations presenting inadequate noise/signals ratio were excluded. Automated spike detection was executed by setting a threshold of 2.5xbaseline for each zebrafish. The number of events and frequency (events/minute) were automatically calculated.

RNA sequencing.

A pool of n= 70 zebrafish larvae (120 hpf) constituted one sample. For each experimental condition (CTRL, 0.1 and 1000 µg/L glyphosate exposure) samples were generated and analyzed in triplicate (total of 9 samples). Total RNA was extracted using Trizol (Invitrogen) and sequenced using a NovaSeq 6000 (Illumina) at the GenomiX platform at the Institute for Functional Genomics. See Extended Method section for details.

Statistical analyses.

Analyses were performed using GraphPad Prism 8.0. When data fulfilled the criteria for applying a parametric test, one-way ANOVA was used followed by Dunnett's multiple comparisons test. Otherwise, Kruskal-Wallis (non-parametric) followed by Dunn's multiple comparisons test was applied ($p < 0.05$). Cumulative hatching rate and microglial morphology were analyzed using two-way ANOVA followed by Dunnett's multiple comparisons test ($p < 0.05$). Asterisks indicate statistical difference compared control group (CTRL): * ($p < 0.05$), ** ($p < 0.01$), *** ($p < 0.001$), **** ($p < 0.0001$). Data are reported as means \pm SD (Standard Deviation)

using violin plots, except the tap-elicited startle reflex test which is showed as mean \pm SEM. RNA-seq statistical analysis is described in the Extended Methods section.

Results

Dose-dependent impact of glyphosate on zebrafish larvae locomotor behavior and in vivo neurophysiology.

From 1.5 to 120 hpf, zebrafish larvae were systematically exposed to a range of glyphosate concentrations (0.05, 0.1, 0.5, 1, 10, 100, 1000, 10.000 µg/L). We screened hatching rates and morphological parameters including head-body length, swimming bladder area, eye diameter and trunk-head angle (Figure 1A). No significant morphological differences were observed at any of the glyphosate concentrations tested (Figure 1B). We report a trend decrease of hatching rates at 72 hpf, although by 96 hpf no difference was observed (Figure 1A). Furthermore, we did not observe any increase in mortality following exposure to glyphosate (*data not shown*). Behavioral analyses performed at 120 hpf revealed defects in locomotor activity at glyphosate concentrations equal or higher than 1000 µg/L (Figure 2). In particular, distance, mean velocity, number of rotations, and body mobility were all decreased (Figure 2B, C, E, F and G). Dosages lower than 10 µg/L did not elicit significant behavioral changes. A tap stimulus test was also performed to study the provoked startle reflex. No significant differences were found when quantifying distance travelled (Supplemental Figure 1A) and maximum velocity (Supplemental Figure 1B) post-stimulus, suggesting a preserved muscular reactivity. Furthermore, phalloidin staining of F-actin in the skeletal muscles (examples in Figure 3A - 3A3) ruled out muscular malformations as a cause of the observed behavioral deficits when testing specific low (0.1µg/L, EU water limits) and high ($\geq 1000\mu\text{g/L}$, eliciting behavioral changes, see Figure 2) glyphosate concentrations. Specifically, quantification of muscle fiber length (µm) indicated no differences across conditions [CTRL (75.97 ± 6.65), low 0.1 µg/L glyphosate (78.57 ± 4.89), high 1000 µg/L (80.94

± 4.44) and 10000 µg/L glyphosate (80.30 ± 2.03), one-way ANOVA, p=0.1908]. Collectively, these data indicate that high glyphosate exposure significantly impairs locomotor behavioral activity and this outcome was not the result of defective skeletal muscle development.

Next, using a *Tg(HuC:Tomato)* zebrafish reporter line we examined whether glyphosate exposure affects brain neuronal structures (examples in Figure 3B-B2). We specifically tested low 0.1µg/L and high, behavior-modifying, 1000µg/L glyphosate concentrations. No significant changes were found for optic nerve length [CTRL (138.0 ± 4.52), 0.1 µg/L glyphosate (139.7 ±2.09), 1000 µg/L glyphosate (140.2 ± 6.08), one-way ANOVA, p=0.4389], optic nerve thickness [CTRL (10.89 ± 0.55), 0.1 µg/L glyphosate (11.35 ± 0.52), 1000 µg/L glyphosate (12.00 ± 1.41), Kruskal – Wallis, H₂=5.011], optic tectum length [CTRL (136.4 ± 11.56), 0.1 ug/L glyphosate (148.4 ± 4.64), 1000 µg/L glyphosate (137.3 ± 7.42), one-way ANOVA, p=0.0820] and length of the 1st hindbrain axon projection [CTRL (188.0 ± 10.87), 0.1 µg/L glyphosate (201.6 ± 16.14), 1000 µg/L glyphosate (192.5 ± 12.10), Kruskal-Wallis, H₂=2.550]. Our analysis rules out the implication of gross neuronal structural malformations in the brain as a potential element underlying behavioral defects.

Finally, we monitored neuronal activity by means of extracellular field recordings in the midbrain of zebrafish exposed to glyphosate, again focusing on 0.1 µg/L and 1000 µg/L glyphosate. We observed a significant increase of spike activity (events/minute) at 1000 µg/L, but not at 0.1 µg/L, as compared to control conditions (Figure 3C1). Spike activity was highly variable at 1000 µg/L glyphosate (Figure 3C1, 3D1, 3D2). Taken together, these data indicate that the defective locomotor

behavioral activity observed following exposure to high glyphosate is underlined by disturbances in neuronal physiology, as measured at the extracellular field potential level.

Impact of glyphosate on glio-cerebrovascular structures imaged in living zebrafish larvae.

To further examine the possibility of structural brain malformations, we reconstructed the tri-dimensional cerebrovascular architecture of *Tg(fli1a:GFP)y1Tg* transgenic zebrafish using *in vivo* 2-photon microscopy (Figure 4; Supplemental Movie 1). We examined the effect of low (0.1 µg/L) and of the behavior-modifying (Figures 2-3; 1000 µg/L) glyphosate concentrations. Figure 4A-A1 provides examples for the entire midbrain Z-stack images. 3D skeleton analysis (Figure 4B-B1) of the *Tg(fli1a:GFP)y1Tg* cerebrovascular tree indicate that glyphosate exposures during larval stages did not modify the midbrain total vascular length (Figure 4C), distribution counts of individual segment lengths (Figure 4D to 4D3) and volumes (Figure 4E to 4E3).

We next examined glial cell morphology by using *Tg(mpeg1:mCherry)* zebrafish larvae, specifically focusing on microglia. Existing evidence indicates activation of microglial cells as a hallmark of neuro-inflammation and a contributing factor to negative neurological outcomes (Beumer et al., 2012; Hanamsagar and Bilbo, 2017). Here, we report morphological signs of microglia reactivity (Mosser et al., 2017; Ransohoff and Perry, 2009; Thion and Garel, 2017; Wolf et al., 2017) in response to low and high glyphosate concentrations (Figure 5; see Supplemental

Movie 2 for a 3D view of a ROI). Following glyphosate exposure, we found a significant percentage increase of cells presenting with a reactive or amoeboid morphology, specifically with enlarged soma and short processes (Figure 5B1, 5B2; see Supplemental Movie 4 for individual cell details). We report a decreased number of resting microglia (Figure 5D) as compared to CTRL. Resting cells presented with a typical small soma and distinct networks of fine ramifications (Figure 5B; see Supplemental Movie 3 for individual cell details). We did not find any difference in the total number of microglia (Figure 5C). Next, by crossing *Tg(fli1a:GFP)y1Tg* and *Tg(mpeg1:mCherry)* zebrafish we were able to examine the position of microglia in relation to the cerebrovasculature (Figure 6A, 6B). Examples of perivascular and parenchymal microglial cells are shown in Figure 6C, 6D. Imaris 3D analysis indicated no changes in the number and the area of juxtaposed microglial cells at vessels in living zebrafish larvae exposed to glyphosate (Figure 6E, 6F). Collectively, these results point to the absence of neurovascular malformations while unveiling microglia morphological reactivity in response to glyphosate exposure.

Transcriptomic-level deregulations in response to glyphosate exposure.

RNA sequencing analysis was performed to unveil candidate pathways and potential molecular links to the reported neurophysiological and cellular changes. As compared to control, exposure to low 0.1 µg/L and high 1000 µg/L glyphosate led to the differential expression of 4774 and 7067 genes respectively. Gene Ontology (GO) analysis was performed for three categories: molecular functions, biological processes and cellular components (complete data are provided in Supplemental Tables 1 – 9). Figure 7 provides two examples of fairy lights graphs indicating the

differentially expressed genes sorted according to molecular functions and biological processes for control vs. 1000 µg/L glyphosate. See Supplemental Figures 2 – 3 for all fairy lights graphs (0.1 µg/L glyphosate and 0.1 vs. 1000 µg/L glyphosate comparisons). The complete GO analysis is provided in Supplemental Tables 1 – 9.

Statistical analysis of GO processes for 0.1 µg/L and 1000 µg/L glyphosate exposure showed that 61 and 52 biological processes, 35 and 36 molecular functions, 17 and 28 cellular components were modified, respectively, by these treatments (Supplemental Tables 1, 2, 3 and 4, 5, 6). The ten most significantly deregulated biological processes and molecular functions are listed in Tables 1 and 2 (for 0,1 and 1000 µg/L glyphosate) together with the 5 most significantly up or downregulated genes ($p < 0.001$). In support of our *in vivo* analyses, we were able to identify deregulated gene families involved in synaptic transmission, synapse organizations, and ion channel activity (Table 1). When we compared 0.1 µg/L to 1000 µg/L glyphosate exposure, we identified 2519 genes which were differentially expressed between these 2 concentrations. A total of 87 biological processes, 49 molecular functions and 26 cellular components were modified (Supplemental Tables 6, 7, 8). Table 3 indicates the 10 most deregulated biological processes and molecular functions, along with the 5 most significantly up or downregulated genes ($p < 0.001$). Taken together, these results indicate changes in the transcriptome caused by both low and high glyphosate exposure in the zebra fish larvae.

Discussion

By exposing zebrafish larvae to varying glyphosate concentrations, we report behavioral modifications at levels equal and higher than 1000 µg/L, accompanied by abnormal spike activity in the midbrain. Low, and environmentally relevant, glyphosate concentrations did not elicit behavioral and neurophysiological changes in these experimental conditions. The neurological outcome observed at high concentrations was not associated with anatomical and neurovascular malformations. When narrowing our target concentrations, we report that low 0,1 µg/L and high 1000 µg/L glyphosate levels induce midbrain microglia morphological reactivity, disclosing a hypothetical role for neuro-inflammation in contributing to behavioral defects in these specific conditions. Finally, our RNAseq data reveals a transcript level imprint at both low and high glyphosate concentrations, in particular the dysregulation of gene families or pathways involved in neuronal functions and synaptic transmission. If observing a clear-cut neurological phenotype requires the exposure to high glyphosate concentrations, at the cellular and transcript levels extra-physiological elements are present in response to low glyphosate exposure, perhaps representing vulnerability risk factors.

Glyphosate and neurological risks: environmental, experimental and clinical clues.

We outline neurological defects specifically at high glyphosate concentration in zebrafish larvae and in the absence of gross or neurovascular malformations. Previous studies indicated a reduction in the swimming distance in zebrafish larvae exposed to 0.01 and 0.5 mg/L glyphosate (Bridi et al., 2017). These results are relevant, as the risk for glyphosate environmental peak contamination and secondary or occupational exposure to humans is not negligible. Importantly, the American

Department of Agriculture and the Environmental Protection Agency indicate that two-thirds of the total glyphosate based herbicides so far produced were applied to the environment in the past decade only (Myers et al., 2016).

We recognize that relevance of the available experimental data to human health is anything but proven. Although epidemiological evidence supports a link between pesticides exposure and neurodevelopmental disorders (Hernández et al., 2016; Roberts et al., 2019; Von Ehrenstein et al., 2019), whether glyphosate may directly contribute to neurological sequel in humans needs further and significant investigation. A recent study points to a moderate level of evidence when associating glyphosate with autism spectrum disorders in humans (Ongono et al., 2020). One study indicates that prenatal or infant exposure to glyphosate, due to proximity to pesticides environmental sources, was associated with increased risk for autism spectrum disorders (Von Ehrenstein et al., 2019). Moreover, excess of attention deficit and hyperactivity disorder was described in children whose parents had glyphosate exposure (De Araujo et al., 2016). In the same work, however, the authors point to insufficient data supporting a public concern for glyphosate-based pesticides and developmental risks (De Araujo et al., 2016). An association between children presenting with attention-deficit disorders and the use of glyphosate from farm families has also been reported (Garry et al., 2002). However, in the latter studies the levels and frequency of glyphosate exposure were not studied, therefore impeding a clear-cut examination and understanding of the link between environmental and human health risks. Existing data suggest that levels of glyphosate in humans are generally low, although high-exposure episodes cannot be excluded (Gillezeau et al., 2019; Soukup et al., 2020). From an experimental

standpoint, glyphosate exposure in rodents negatively impacts neuronal functions and behavior, although at concentrations higher than the acceptable daily intake (Cattani et al., 2017; Gallegos et al., 2016). Finally, maternal exposure to high levels of glyphosate was reported to promote autistic-like behavioral defects in murine male offspring (Pu et al., 2020).

Cellular contributors to glyphosate induced neurological defects.

At the dosage examined, our results rule out the presence of neurovascular malformations but do indicate morphological microglial changes, a sign of neuro-inflammation. In this model, the microglial morphological modifications occurred at a low, or environmentally relevant, glyphosate concentration and in the absence of behavioral or electrophysiological phenotypes. Importantly, microglia reactivity during pre and early postnatal development impairs several aspects of brain development (Mosser et al., 2017; Thion and Garel, 2017) and it has been proposed as a risk factor for neurological or psychiatric conditions (Hanamsagar and Bilbo, 2017; Klement et al., 2019, 2018). Microglia reactivity in pathological settings is associated with clear changes in their morphology, with gradual and reversible transitions from ramified cells with a small soma to hypertrophic or amoeboid large cells resembling peripheral macrophages (Hanisch and Kettenmann, 2007; Librizzi et al., 2018; Savage et al., 2019). Only a few studies exist on the consequences of glyphosate exposure on microglial reactivity. In particular, one report indicates that exposure to 250 mg/kg and 500 mg/Kg of glyphosate-based herbicide during pregnancy and lactation leads to microglia reactivity in the hippocampus and prefrontal cortex in the

rodent offspring (Ait-Bali et al., 2020), although this was performed using concentrations above the glyphosate acceptable daily intake (ADI).

Pathways connecting glyphosate to neurological changes: initial clues.

Transcriptomics is proving to be a useful tool for assessing signatures from xenobiotics exposure. Our data provide information on the potential impact of the external environment, supporting the hypothesis of an underlying pesticide-induced cell vulnerability that may anticipate harmful consequences on health (Klement et al., 2020; Pagé-Larivière et al., 2019; Webster and Santos, 2015). Gene ontology analysis of our RNAseq dataset reveals deregulation of gene pathways directly involved in neuronal physiology and synaptic transmission, converging with the negative electrophysiological outcome here reported. For instance, genes coding for glutamate receptor (e.g. *grin2*, *gria3*, *grm4*, *grik5*), GABA receptor activity (e.g. *gabra*, *gabrb*), and cation channels (e.g. *kcnj*, *cacna*) were up-regulated after glyphosate exposure. We also observed deregulation of microglial genes (Lyons and Talbot, 2015) after glyphosate exposure, including downregulation of *irf8* (development of primitive macrophages), downregulation of *mpeg1.2* and *mfap4* (early macrophage gene in microglia). At 1000 µg/L glyphosate, the downregulation of *apoe* (microglia differentiation), *csf1ra* (macrophage migration from the yolk sac to the CNS) and *nlr3l* (microglia development) occurred. Previous studies have shown that glyphosate induces oxidative stress in zebrafish (Sulukan et al., 2017; Webster and Santos, 2015) which supports our own findings that several GO genes related to mitochondria (i.e. transmembrane transport) were altered following glyphosate exposure. Furthermore, adult zebrafish exposed for 7 days to glyphosate-based

herbicides displayed a gene-level mitochondrial dysfunction along with behavioral impairments at 1000 and 10.000 µg/L (Pereira et al., 2018).

Study limitations and conclusions.

The presented research leaves a number of significant queries that should be further examined. Foremost is the significance of data obtained using zebrafish larvae, an ecotoxicological environmental model, to human exposure as it can accidentally or voluntarily occur from contaminated matrices or food. Thus, transitioning from an environmental context to consumers' health risks, specific to perinatal periods, is challenging and no clear-cut approaches exist (Schantz et al., 2020). From a pathophysiological standpoint, the implication of neuro-inflammation during glyphosate exposure remains to be fully defined, including the involvement of astrocytes together with the examination of cell specific soluble inflammatory factors. The latter is important because neuro-inflammation represents a hallmark of brain disorders (Giannoni et al., 2018; Ransohoff and Perry, 2009) and could represent an important link between glyphosate exposure and behavioral adaptations. We here acknowledge that the use of PTU, decreasing pigmentation and allowing 2-photon microscopy, could represent a confounding factor. Supporting the validity of our results and a detrimental effect of glyphosate on microglial cells we here underline that: i) control zebrafish received PTU, indicating that at least PTU alone does not impact microglial cells as compared to glyphosate conditions; ii) we did not find cellular level neurovascular changes across experimental conditions (Figures 3 - 4), supporting cell specificity for the results shown in Figure 5; iii) we report no locomotor modifications when comparing control with PTU zebrafish, specifically distance (mm)

[CTRL (3023 ± 1047), PTU (2965 ± 1512), PTU + 0.1 $\mu\text{g/L}$ glyphosate (3265 ± 1654)] and mean velocity (mm/sec) [CTRL (1.53 ± 0.53), PTU (1.65 ± 0.84), PTU + 0.1 $\mu\text{g/L}$ glyphosate (1.82 ± 0.92)]. We also found no differences between PTU vs. PTU + glyphosate when analyzing morphology and muscle structures (Supplemental Figure 4). Furthermore, recent publications have used PTU in zebrafish embryos to examine microscopy read-outs (Huang et al., 2020; Kocere et al., 2020; Shao et al., 2020). Nevertheless, the possibility of a binary mixture toxicity associated with PTU and the varying glyphosate concentrations cannot be completely excluded. Regarding our behavioral analyses we here acknowledge that, while 4 dpf zebrafish embryos do not respond to an acoustic startle, 5 dpf zebrafish do (Best et al., 2008; Bhandiwad et al., 2013; Zeddies and Fay, 2005) and they were used by others when testing chemicals (García-González et al., 2020; Wolman et al., 2011).

Although our data outline transcriptome changes at low glyphosate concentrations (0.1 $\mu\text{g/L}$), we were unable to detect physiological level changes in the assays we have performed as compared to untreated controls. Further analysis will be required targeting those specific genes, identified in our dataset, that are directly implicated in the phenotypes here reported. Follow-up studies should include the generation of specific knock-out zebrafish lines along with quantitative confirmation of specific gene levels in response to environmental contaminants. Confirmatory protein level analyses are undoubtedly required to understand the mechanisms by which low glyphosate exposure could contribute to a vulnerable condition, and perhaps to more subtle neurological phenotypes compared to those associated with high concentrations.

In conclusion, our results provide a set of novel data outlining the dose-dependent impact of glyphosate to the zebrafish larval brain. This research could be further developed to decipher whether a causal link may exists between the exposure to a relevant herbicide and risks for neurological defects, or adaptations, in humans.

References

- Ait-Bali, Y., Ba-M'hamed, S., Gambarotta, G., Sassoè-Pognetto, M., Giustetto, M., Bennis, M., 2020. Pre- and postnatal exposure to glyphosate-based herbicide causes behavioral and cognitive impairments in adult mice: evidence of cortical ad hippocampal dysfunction. *Arch. Toxicol.* 94, 1703–1723. doi:10.1007/s00204-020-02677-7
- Annett, R., Habibi, H.R., Hontela, A., 2014. Impact of glyphosate and glyphosate-based herbicides on the freshwater environment. *J. Appl. Toxicol.* 34, 458–479. doi:10.1002/jat.2997
- Baraban, S.C., 2013. Forebrain electrophysiological recording in larval zebrafish. *J. Vis. Exp.* doi:10.3791/50104
- Benbrook, C.M., 2016. Trends in glyphosate herbicide use in the United States and globally. *Environ. Sci. Eur.* 28, 1–15. doi:10.1186/s12302-016-0070-0
- Bernut, A., Herrmann, J.L., Kissa, K., Dubremetz, J.F., Gaillard, J.L., Lutfalla, G., Kremer, L., 2014. Mycobacterium abscessus cording prevents phagocytosis and promotes abscess formation. *Proc. Natl. Acad. Sci. U. S. A.* 111. doi:10.1073/pnas.1321390111
- Best, J.D., Berghmans, S., Hunt, J.J.F.G., Clarke, S.C., Fleming, A., Goldsmith, P., Roach, A.G., 2008. Non-associative learning in larval zebrafish. *Neuropsychopharmacology* 33, 1206–1215. doi:10.1038/sj.npp.1301489
- Beumer, W., Gibney, S.M., Drexhage, R.C., Pont-Lezica, L., Doorduyn, J., Klein, H.C., Steiner, J., Connor, T.J., Harkin, A., Versnel, M.A., Drexhage, H.A., 2012. The immune theory of psychiatric diseases: a key role for activated microglia and circulating monocytes. *J. Leukoc. Biol.* 92, 959–975. doi:10.1189/jlb.0212100
- Bhandiwad, A.A., Zeddies, D.G., Raible, D.W., Rubel, E.W., Sisneros, J.A., 2013. Auditory sensitivity of larval zebrafish (*Danio rerio*) measured using a behavioral prepulse inhibition assay. *J. Exp. Biol.* 216, 3504–3513. doi:10.1242/jeb.087635
- Bridi, D., Altenhofen, S., Gonzalez, J.B., Reolon, G.K., Bonan, C.D., 2017. Glyphosate and Roundup® alter morphology and behavior in zebrafish. *Toxicology* 392, 32–39. doi:10.1016/j.tox.2017.10.007
- Canada Health, 2019. Guidelines for Canadian Drinking Water Quality - Summary Table. Ottawa, Canada.

- Carles, L., Gardon, H., Joseph, L., Sanchís, J., Farré, M., Artigas, J., 2019. Meta-analysis of glyphosate contamination in surface waters and dissipation by biofilms. *Environ. Int.* 124, 284–293. doi:10.1016/j.envint.2018.12.064
- Cattani, D., Cesconetto, P.A., Tavares, M.K., Parisotto, E.B., De Oliveira, P.A., Rieg, C.E.H., Leite, M.C., Prediger, R.D.S., Wendt, N.C., Razzera, G., Filho, D.W., Zamoner, A., 2017. Developmental exposure to glyphosate-based herbicide and depressive-like behavior in adult offspring: Implication of glutamate excitotoxicity and oxidative stress. *Toxicology* 387, 67–80. doi:10.1016/j.tox.2017.06.001
- De Araujo, J.S.A., Delgado, I.F., Paumgartten, F.J.R., 2016. Glyphosate and adverse pregnancy outcomes, a systematic review of observational studies. *BMC Public Health*. doi:10.1186/s12889-016-3153-3
- Gallegos, C.E., Bartos, M., Bras, C., Gumilar, F., Antonelli, M.C., Minetti, A., 2016. Exposure to a glyphosate-based herbicide during pregnancy and lactation induces neurobehavioral alterations in rat offspring. *Neurotoxicology* 53, 20–28. doi:10.1016/j.neuro.2015.11.015
- García-González, J., Brock, A.J., Parker, M.O., Riley, R.J., Joliffe, D., Sudwarts, A., Teh, M.T., Busch-Nentwich, E.M., Stemple, D.L., Martineau, A.R., Kaprio, J., Palviainen, T., Kuan, V., Walton, R.T., Brennan, C.H., 2020. Identification of slit3 as a locus affecting nicotine preference in zebrafish and human smoking behaviour. *Elife* 9. doi:10.7554/eLife.51295
- Garry, V.F., Harkins, M.E., Erickson, L.L., Long-Simpson, L.K., Holland, S.E., Burroughs, B.L., 2002. Birth defects, season of conception, and sex of children born to pesticide applicators living in the Red River Valley of Minnesota, USA. *Environ. Health Perspect.* 110, 441–449. doi:10.1289/ehp.02110s3441
- Giannoni, P., Badaut, J., Dargazanli, C., De Maudave, A.F., Klement, W., Costalat, V., Marchi, N., 2018. The pericyte–glia interface at the blood–brain barrier. *Clin. Sci.* 132, 361–374. doi:10.1042/CS20171634
- Gillezeau, C., Van Gerwen, M., Shaffer, R.M., Rana, I., Zhang, L., Sheppard, L., Taioli, E., 2019. The evidence of human exposure to glyphosate: a review. *Environ. Heal.* 18. doi:10.1186/s12940-018-0435-5
- Han, E., Ho Oh, K., Park, S., Chan Rah, Y., Park, H.C., Koun, S., Choi, J., 2020. Analysis of behavioral changes in zebrafish (*Danio rerio*) larvae caused by aminoglycoside-induced damage to the lateral line and muscles. *Neurotoxicology* 78, 134–142. doi:10.1016/j.neuro.2020.03.005

- Hanamsagar, R., Bilbo, S.D., 2017. Environment matters: microglia function and dysfunction in a changing world. *Curr. Opin. Neurobiol.* doi:10.1016/j.conb.2017.10.007
- Hanisch, U.K., Kettenmann, H., 2007. Microglia: Active sensor and versatile effector cells in the normal and pathologic brain. *Nat. Neurosci.* doi:10.1038/nn1997
- Hanke, I., Wittmer, I., Bischofberger, S., Stamm, C., Singer, H., 2010. Relevance of urban glyphosate use for surface water quality. *Chemosphere* 81, 422–429. doi:10.1016/j.chemosphere.2010.06.067
- Hernández, A.F., González-Alzaga, B., López-Flores, I., Lacasaña, M., 2016. Systematic reviews on neurodevelopmental and neurodegenerative disorders linked to pesticide exposure: Methodological features and impact on risk assessment. *Environ. Int.* 92–93, 657–679. doi:10.1016/j.envint.2016.01.020
- Huang, Y., Ma, J., Meng, Y., Wei, Y., Xie, S., Jiang, P., Wang, Z., Chen, X., Liu, Z., Zhong, K., Cao, Z., Liao, X., Xiao, J., Lu, H., 2020. Exposure to Oxadiazon-Butachlor causes cardiac toxicity in zebrafish embryos. *Environ. Pollut.* 265, 114775. doi:10.1016/j.envpol.2020.114775
- Jia, S., Wu, X., Wu, Y., Cui, X., Tao, B., Zhu, Z., Hu, W., 2020. Multiple developmental defects in sox11a mutant zebrafish with features of coffin-siris syndrome. *Int. J. Biol. Sci.* 16, 3039–3049. doi:10.7150/ijbs.47510
- Kimmel, C.B., Ballard, W.W., Kimmel, S.R., Ullmann, B., Schilling, T.F., 1995. Stages of embryonic development of the zebrafish. *Dev. Dyn.* 203, 253–310. doi:10.1002/aja.1002030302
- Klement, W., Blaquiere, M., Zub, E., deBock, F., Boux, F., Barbier, E., Audinat, E., Lerner-Natoli, M., Marchi, N., 2019. A pericyte-glia scarring develops at the leaky capillaries in the hippocampus during seizure activity. *Epilepsia* 60, epi.16019. doi:10.1111/epi.16019
- Klement, W., Garbelli, R., Zub, E., Rossini, L., Tassi, L., Girard, B., Blaquiere, M., Bertaso, F., Perroy, J., de Bock, F., Marchi, N., 2018. Seizure progression and inflammatory mediators promote pericytosis and pericyte-microglia clustering at the cerebrovasculature. *Neurobiol. Dis.* 113, 70–81. doi:10.1016/j.nbd.2018.02.002
- Klement, W., Oliviero, F., Gangarossa, G., Zub, E., De Bock, F., Forner, I., Blaquiere, M., Lasserre, F., Pascussi, J.-M., Maurice, T., Audinat, E., Ellero-Simatos, S., Gamet-Payrastre, L., Mselli-Lakhal, L., Marchi, N., 2020. Life-long dietary

pesticides cocktail induces astrogliosis along with behavioral adaptations and activates p450 metabolic pathways. *Neuroscience*. doi:10.1016/j.neuroscience.2020.07.039

Kocere, A., Resseguier, J., Wohlmann, J., Skjeldal, F.M., Khan, S., Speth, M., Dal, N.J.K., Ng, M.Y.W., Alonso-Rodriguez, N., Scarpa, E., Rizzello, L., Battaglia, G., Griffiths, G., Fenaroli, F., 2020. Real-time imaging of polymersome nanoparticles in zebrafish embryos engrafted with melanoma cancer cells: Localization, toxicity and treatment analysis. *EBioMedicine* 58, 102902. doi:10.1016/j.ebiom.2020.102902

Landrigan, P.J., Belpoggi, F., 2018. The need for independent research on the health effects of glyphosate-based herbicides. *Environ. Heal. A Glob. Access Sci. Source*. doi:10.1186/s12940-018-0392-z

Librizzi, L., de Cutis, M., Janigro, D., Runtz, L., de Bock, F., Barbier, E.L., Marchi, N., 2018. Cerebrovascular heterogeneity and neuronal excitability. *Neurosci. Lett*. doi:10.1016/j.neulet.2017.01.013

Lyons, D.A., Talbot, W.S., 2015. Glial cell development and function in zebrafish. *Cold Spring Harb. Perspect. Biol.* 7. doi:10.1101/cshperspect.a020586

Mosser, C.A., Baptista, S., Arnoux, I., Audinat, E., 2017. Microglia in CNS development: Shaping the brain for the future. *Prog. Neurobiol*. doi:10.1016/j.pneurobio.2017.01.002

Myers, J.P., Antoniou, M.N., Blumberg, B., Carroll, L., Colborn, T., Everett, L.G., Hansen, M., Landrigan, P.J., Lanphear, B.P., Mesnage, R., Vandenberg, L.N., Vom Saal, F.S., Welshons, W. V., Benbrook, C.M., 2016. Concerns over use of glyphosate-based herbicides and risks associated with exposures: A consensus statement. *Environ. Heal. A Glob. Access Sci. Source*. doi:10.1186/s12940-016-0117-0

Niemann, L., Sieke, C., Pfeil, R., Solecki, R., 2015. A critical review of glyphosate findings in human urine samples and comparison with the exposure of operators and consumers. *J. fur Verbraucherschutz und Leb*. doi:10.1007/s00003-014-0927-3

Ongono, J.S., Béranger, R., Baghdadli, A., Mortamais, M., 2020. Pesticides used in Europe and autism spectrum disorder risk: can novel exposure hypotheses be formulated beyond organophosphates, organochlorines, pyrethroids and carbamates? - A systematic review. *Environ. Res*.

doi:10.1016/j.envres.2020.109646

Pagé-Larivière, F., Crump, D., O'Brien, J.M., 2019. Transcriptomic points-of-departure from short-term exposure studies are protective of chronic effects for fish exposed to estrogenic chemicals. *Toxicol. Appl. Pharmacol.* 378, 114634. doi:10.1016/j.taap.2019.114634

Pereira, A.G., Jaramillo, M.L., Remor, A.P., Latini, A., Davico, C.E., da Silva, M.L., Müller, Y.M.R., Ammar, D., Nazari, E.M., 2018. Low-concentration exposure to glyphosate-based herbicide modulates the complexes of the mitochondrial respiratory chain and induces mitochondrial hyperpolarization in the *Danio rerio* brain. *Chemosphere* 209, 353–362. doi:10.1016/j.chemosphere.2018.06.075

Perry, V.H., Nicoll, J.A.R., Holmes, C., 2010. Microglia in neurodegenerative disease. *Nat. Rev. Neurol.* doi:10.1038/nrneurol.2010.17

Pu, Y., Yang, J., Chang, L., Qu, Y., Wang, S., Zhang, K., Xiong, Z., Zhang, J., Tan, Y., Wang, X., Fujita, Y., Ishima, T., Wang, D., Hwang, S.H., Hammock, B.D., Hashimoto, K., 2020. Maternal glyphosate exposure causes autism-like behaviors in offspring through increased expression of soluble epoxide hydrolase. *Proc. Natl. Acad. Sci. U. S. A.* 117, 11753–11759. doi:10.1073/pnas.1922287117

Ransohoff, R.M., Perry, V.H., 2009. Microglial physiology: Unique stimuli, specialized responses. *Annu. Rev. Immunol.* doi:10.1146/annurev.immunol.021908.132528

Roberts, J.R., Dawley, E.H., Reigart, J.R., 2019. Children's low-level pesticide exposure and associations with autism and ADHD: a review. *Pediatr. Res.* doi:10.1038/s41390-018-0200-z

Roy, N.M., Carneiro, B., Ochs, J., 2016. Glyphosate induces neurotoxicity in zebrafish. *Environ. Toxicol. Pharmacol.* 42, 45–54. doi:10.1016/j.etap.2016.01.003

Sandrini, J.Z., Rola, R.C., Lopes, F.M., Buffon, H.F., Freitas, M.M., Martins, C. de M.G., da Rosa, C.E., 2013. Effects of glyphosate on cholinesterase activity of the mussel *Perna perna* and the fish *Danio rerio* and *Jenynsia multidentata*: *In vitro* studies. *Aquat. Toxicol.* 130–131, 171–173. doi:10.1016/j.aquatox.2013.01.006

Savage, J.C., Carrier, M., Tremblay, M.È., 2019. Morphology of microglia across contexts of health and disease, in: *methods in molecular biology*. Humana Press Inc., pp. 13–26. doi:10.1007/978-1-4939-9658-2_2

Schantz, S.L., Eskenazi, B., Buckley, J.P., Braun, J.M., Sprowles, J.N., Bennett, D.H., Cordero, J., Frazier, J.A., Lewis, J., Hertz-Picciotto, I., Lyall, K., Nozadi, S.S., Sagiv, S., Stroustrup, A.M., Volk, H.E., Watkins, D.J., 2020. A framework for assessing the impact of chemical exposures on neurodevelopment in ECHO: Opportunities and challenges. *Environ. Res.* doi:10.1016/j.envres.2020.109709

Scribner, E.A., Battaglin, W.A., Gilliom, R.J., Meyer, M.T., 2007. Concentrations of glyphosate, its degradation product, aminomethylphosphonic acid, and glufosinate in ground-and surface-water, rainfall, and soil samples collected in the United States, 2001-06 Scientific Investigations Report 2007-5122. Virginia.

Sealey, L.A., Hughes, B.W., Sriskanda, A.N., Guest, J.R., Gibson, A.D., Johnson-Williams, L., Pace, D.G., Bagasra, O., 2016. Environmental factors in the development of autism spectrum disorders. *Environ. Int.* doi:10.1016/j.envint.2015.12.021

Shao, W., Zhong, D., Jiang, H., Han, Y., Yin, Y., Li, R., Qian, X., Chen, D., Jing, L., 2020. A new aminoglycoside etimicin shows low nephrotoxicity and ototoxicity in zebrafish embryos. *J. Appl. Toxicol.* jat.4093. doi:10.1002/jat.4093

Snow, C.J., Peterson, M.T., Khalil, A., Henry, C.A., 2008. Muscle development is disrupted in zebrafish embryos deficient for fibronectin. *Dev. Dyn.* 237, 2542–2553. doi:10.1002/dvdy.21670

Soukup, S.T., Merz, B., Bub, A., Hoffmann, I., Watzl, B., Steinberg, P., Kulling, S.E., 2020. Glyphosate and AMPA levels in human urine samples and their correlation with food consumption: results of the cross-sectional KarMeN study in Germany. *Arch. Toxicol.* 94, 1575–1584. doi:10.1007/s00204-020-02704-7

Sulukan, E., Köktürk, M., Ceylan, H., Beydemir, Ş., Işık, M., Atamanalp, M., Ceyhun, S.B., 2017. An approach to clarify the effect mechanism of glyphosate on body malformations during embryonic development of zebrafish (*Danio rerio*). *Chemosphere* 180, 77–85. doi:10.1016/j.chemosphere.2017.04.018

Székács, A., Darvas, B., 2018. Re-registration challenges of glyphosate in the European Union. *Front. Environ. Sci.* 6, 78. doi:10.3389/fenvs.2018.00078

Thion, M.S., Garel, S., 2017. On place and time: microglia in embryonic and perinatal brain development. *Curr. Opin. Neurobiol.* doi:10.1016/j.conb.2017.10.004

Uren Webster, T.M., Laing, L. V, Florance, H., Santos, E.M., 2013. Effects of glyphosate and its formulation, Roundup, on reproduction in zebrafish (*Danio rerio*). doi:10.1021/es404258h

- Van Bruggen, A.H.C., He, M.M., Shin, K., Mai, V., Jeong, K.C., Finckh, M.R., Morris, J.G., 2018. Environmental and health effects of the herbicide glyphosate. *Sci. Total Environ.* doi:10.1016/j.scitotenv.2017.10.309
- Vandenberg, L.N., Blumberg, B., Antoniou, M.N., Benbrook, C.M., Carroll, L., Colborn, T., Everett, L.G., Hansen, M., Landrigan, P.J., Lanphear, B.P., Mesnage, R., vom Saal, F.S., Welshons, W. V., Myers, J.P., 2017. Is it time to reassess current safety standards for glyphosate-based herbicides? *J. Epidemiol. Community Health* 71, 613–618. doi:10.1136/jech-2016-208463
- Von Ehrenstein, O.S., Ling, C., Cui, X., Cockburn, M., Park, A.S., Yu, F., Wu, J., Ritz, B., 2019. Prenatal and infant exposure to ambient pesticides and autism spectrum disorder in children: Population based case-control study. *BMJ* 364, 962. doi:10.1136/bmj.l962
- Webster, T.M.U., Santos, E.M., 2015. Global transcriptomic profiling demonstrates induction of oxidative stress and of compensatory cellular stress responses in brown trout exposed to glyphosate and Roundup. *BMC Genomics* 16, 1–14. doi:10.1186/s12864-015-1254-5
- Wolf, S.A., Boddeke, H.W.G.M., Kettenmann, H., 2017. Microglia in physiology and disease. *Annu. Rev. Physiol.* doi:10.1146/annurev-physiol-022516-034406
- Wolman, M.A., Jain, R.A., Liss, L., Granato, M., 2011. Chemical modulation of memory formation in larval zebrafish. *Proc. Natl. Acad. Sci. U. S. A.* 108, 15468–15473. doi:10.1073/pnas.1107156108
- Zeddies, D.G., Fay, R.R., 2005. Development of the acoustically evoked behavioral response in zebrafish to pure tones. *J. Exp. Biol.* 208, 1363–1372. doi:10.1242/jeb.01534
- Zhang, S., Xu, J., Kuang, X., Li, S., Li, X., Chen, D., Zhao, X., Feng, X., 2017. Biological impacts of glyphosate on morphology, embryo biomechanics and larval behavior in zebrafish (*Danio rerio*). *Chemosphere* 181, 270–280. doi:10.1016/j.chemosphere.2017.04.094

A

		CTRL	0.05 µg/L	0.1 µg/L	0.5 µg/L	1 µg/L	10 µg/L	100 µg/L	1000 µg/L	10000 µg/L
Hatching rate	72 hpf	73.20 ± 16.70	46.1 ± 7.7 0	63.80 ± 15.50	51.50 ± 20.3	63.80 ± 15.50	51.50 ± 20.30	39.30 ± 14.80	50.40 ± 23.90	62.10 ± 26.40
	96 hpf	98.50 ± 2.60	99.30 ± 1.20	100 ± 0.00	100 ± 0.00	97.80 ± 3.90	100 ± 0.00	94.80 ± 5.10	98.70 ± 1.20	97.60 ± 2.50
Total length (µm)		3717 ± 89.3	3696 ± 94.2	3730 ± 67.2	3730 ± 67.0	3710 ± 40.0	3676 ± 112.9	3738 ± 109.3	3736 ± 59.1	3762 ± 62.9
Swimming bladder area (µm ²)		61955 ± 4388	63331 ± 3172	63023 ± 6547	62653 ± 4355	61320 ± 5652	61930 ± 3973	62309 ± 2714	62089 ± 5004	64713 ± 4389
Eye diameter (µm)		340.2 ± 18.0	325.1 ± 11.5	324.9 ± 18.5	324.8 ± 18.5	325.2 ± 15.6	323.5 ± 12.0	315.6 ± 12.1	325.0 ± 28.4	332.7 ± 8.42
Trunk – head angle (deg)		157.3 ± 4.6	155.4 ± 2.9	156.0 ± 3.3	155.7 ± 2.10	156.8 ± 2.6	155.4 ± 2.3	155.5 ± 1.9	154.5 ± 2.7	157.0 ± 3.3

B

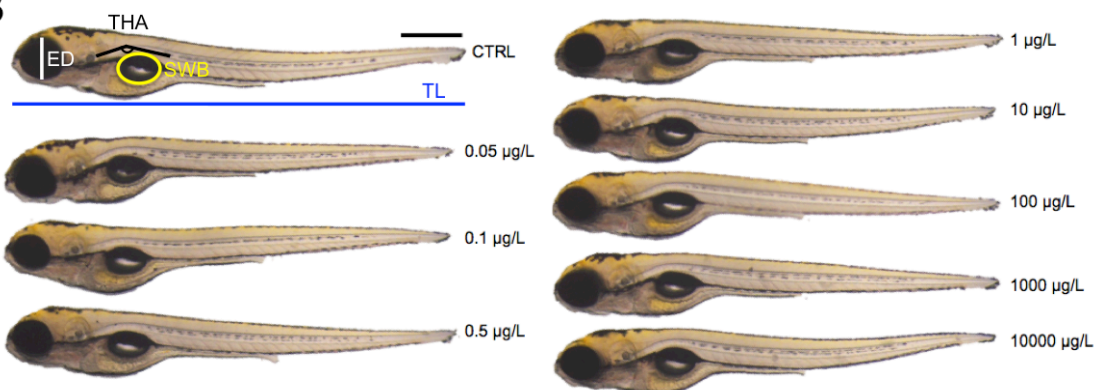


Figure 1. Screening hatching rates and gross morphological parameters at varying glyphosate concentrations. A) Cumulative hatching rate consecutively assessed at 72 and 96 hpf and expressed as hatched eggs / total x 100. Data reported as means ± SD. Experiments conducted in triplicate (n = 150/group; 2-way ANOVA, Dunnett's multiple comparisons test, p < 0.05). Morphological parameters: Total body length (TL, µm), swimming bladder (SWB, µm²), eye diameter (ED, µm) and trunk-head angle (THA, degrees) of zebrafish larvae at 120 hpf (1-way ANOVA, Dunnett's multiple comparisons test, p<0.05). Data reported as means ± SD. Experiments conducted in duplicate (n = 12/group). **B)** Examples for morphological assessments. Scale bar: 500 µm.

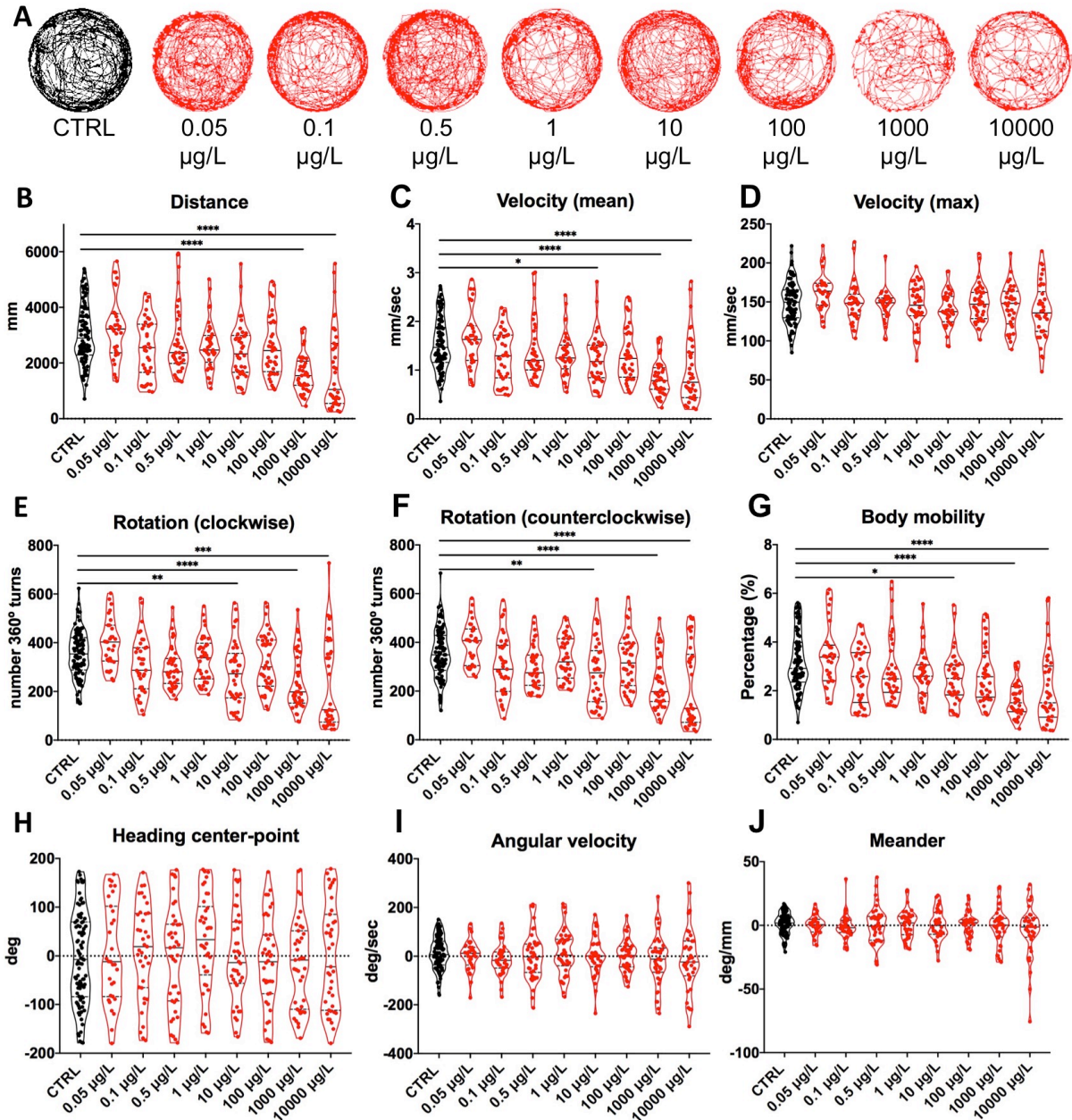


Figure 2. Behavioral defects in zebrafish larvae elicited with increasing glyphosate concentrations. **A)** Examples of 30-minute swimming paths for each experimental group. **B)** Distance in mm; **C)** Mean velocity in mm/sec; **D)** Maximum velocity in mm/sec; **E)** clockwise rotation in number of 360° turns; **F)** counter clockwise rotation in number of 360° turns; **G)** percentage of body mobility; **H)** direction of the body in deg; **I)** angular velocity in deg/sec; **J)** convolution of the movement in deg/mm. Data are reported as mean \pm SD, (1-way ANOVA, Dunnett's multiple comparison test, * $p < 0.05$, ** $p < 0.01$, *** $p < 0.001$, **** $p < 0.0001$). Experiments were performed in duplicate (CTRL $n = 90$, glyphosate groups $n = 40$).

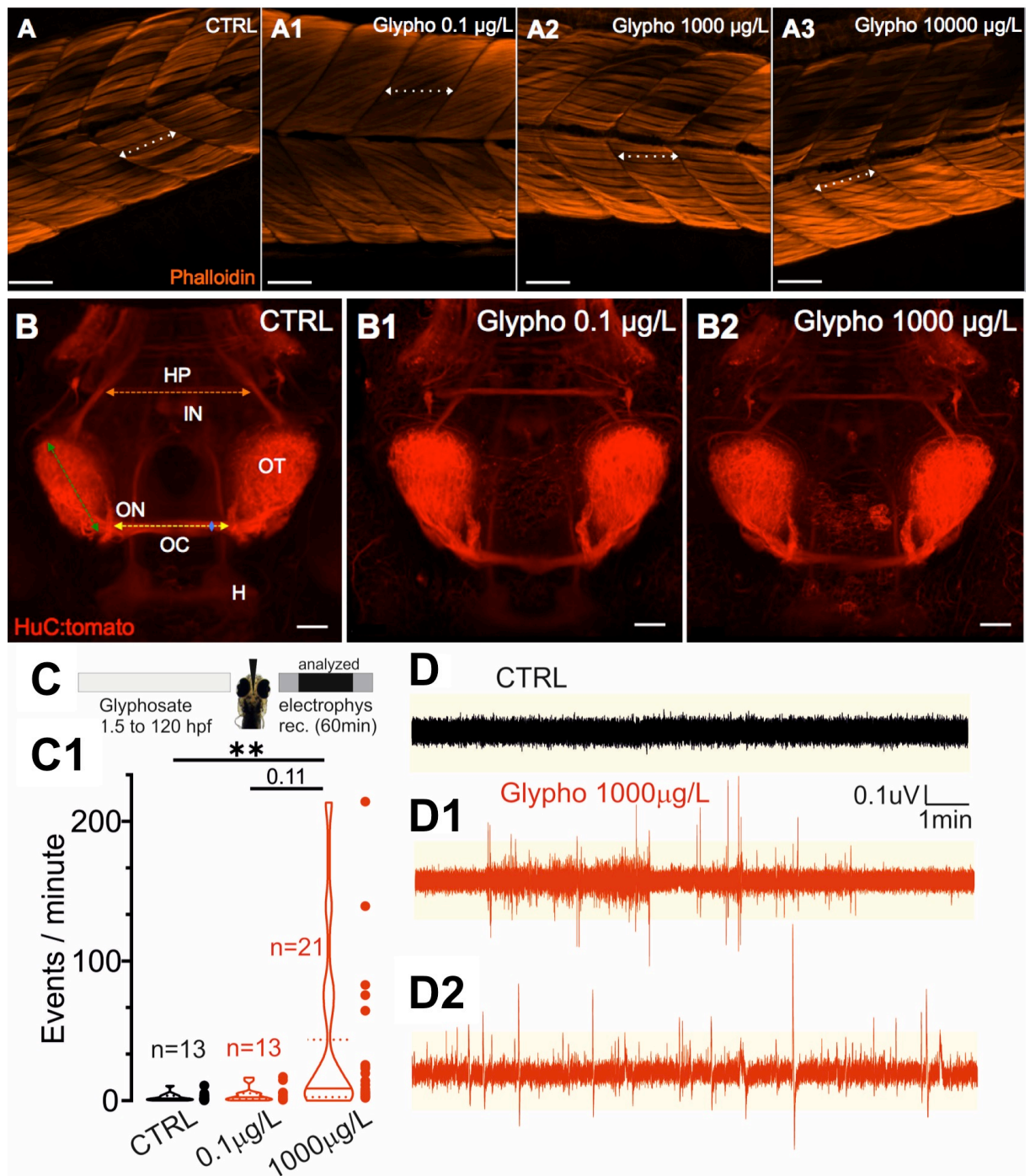


Figure 3. Neurophysiological modifications occur at high glyphosate concentration and in the absence of muscle or neuronal malformations. **A)** Lateral views of trunk somites in zebrafish larvae stained using phalloidin. Examples of CTRL (A), 0.1 µg/L glyphosate (A1), 1000 µg/L glyphosate (A2) and 10000 µg/L glyphosate (A3). Dashed lines with arrows indicated the length of a typical fiber measured. No significant changes were observed (quantifications are provided in the Results). Experiments were conducted in duplicate (n = 7/group). Scale bar: 50 µm. **B)** 2-photon Z-stack images of a pan-neuronal HuC:tomato zebrafish larva showing the principal brain structures in CTRL (B), 0.1 µg/L glyphosate (B1), 1000 µg/L glyphosate (B2). Scale bar: 40 µm. Dorsal view, with the caudal tail up. HP: hindbrain axon projections, IN: interpeduncular nucleus, OT: optic tectum, ON:

917 optic nerve, OC: optic chiasm, H: habenula. Dashed lines with arrows indicate the structures
918 quantified: orange (length of the 1st hindbrain axon projection), green (length of the optic
919 tectum), yellow (length of the optic nerve) and blue (thickness of the optic nerve). No
920 changes were observed (quantifications are provided in the Results). Experiments were
921 conducted in duplicate (n=5/group). **C)** Field potential recordings of the zebrafish midbrain.
922 After glyphosate exposures (light grey rectangle) recording were performed for 1 hour (dark
923 grey rectangle) and analyzed from 10 to 40 minutes (black rectangle). C1) Quantification
924 spike frequency (Kruskall-Wallis, Dunn's multiple comparison test $H_3=9.70$, $p=0.0078$).
925 Asterisk ($p < 0.01$) indicates statistical difference between CTRL and 1000 $\mu\text{g/L}$ glyphosate (n
926 = 13 for CTRL, $n = 13$ for 0.1 $\mu\text{g/L}$, $n = 21$ for 1000 $\mu\text{g/L}$). **D)** Examples of traces of CTRL (D)
927 and 1000 $\mu\text{g/L}$ glyphosate (D1, D2). Yellow shadows indicate the 2.5x threshold used for
928 spike detection.
929
930
931
932
933
934
935
936
937
938

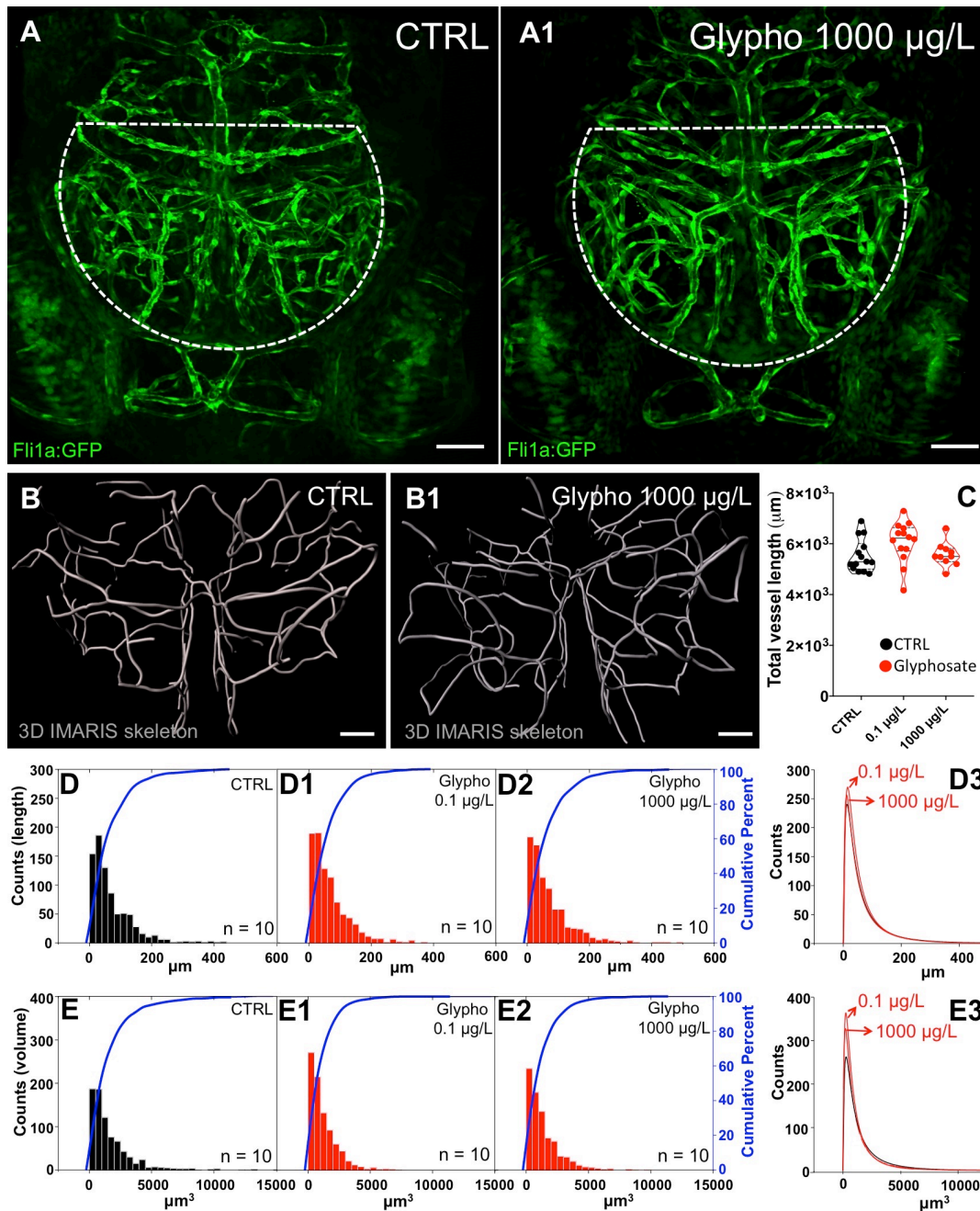


Figure 4. Cerebrovascular structures are preserved during glyphosate exposure. **A)** 2-photon Z-stack reconstructions of a fli1a:GFP zebrafish larva showing the brain vasculature in green for CTRL (A) and 1000 µg/L glyphosate (A1). Scale bar: 50 µm. Dorsal view, with the caudal tail up. See Supplemental Movie 1 for details. A 3D ROI is delimited by a white dashed semi-circle. **B)** Examples of Imaris 3D skeleton reconstruction of the midbrain vasculature for CTRL (B) and 1000 µg/L glyphosate (B1). Scale bar: 30 µm. **C)** Quantification of the total vasculature length (1-way ANOVA, Dunnett's multiple comparisons test, $p < 0.05$). **D)** Histograms of vessels length distribution for CTRL (D), 0.1 µg/L (D1) and 1000 µg/L glyphosate (D2). Blue lines represent the cumulative percentages. Distribution curves are indicated in (D3). **E)** Histograms of vessels volume distribution for CTRL (E), 0.1 µg/L (E1) and 1000 µg/L glyphosate (E2). Distribution curves are indicated in (E3). Data refer to $n=10$ /condition.

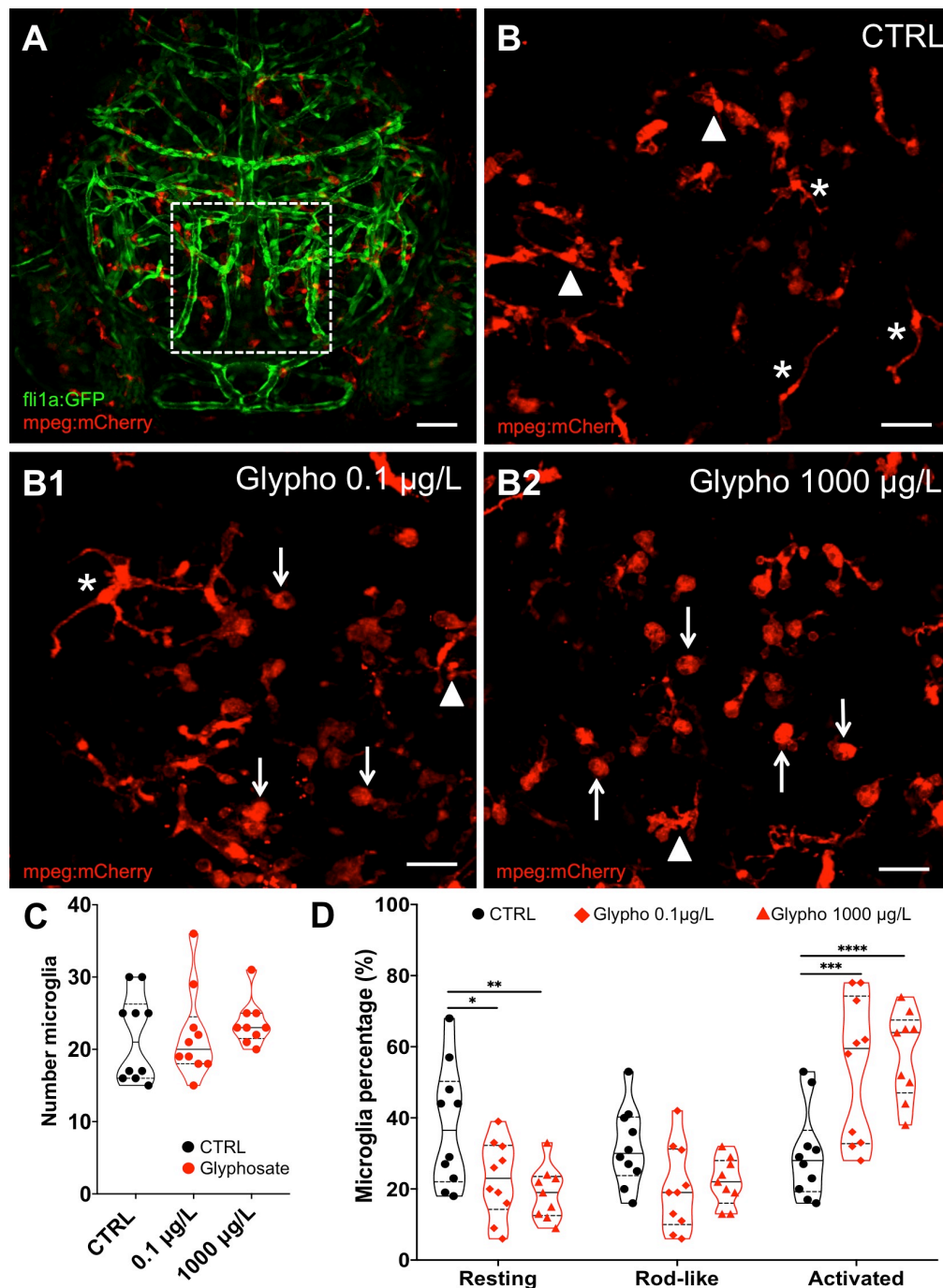


Figure 5. Morphological activation of microglia in response to glyphosate. **A)** 2-photon Z-stack reconstructions of a *fli1a:GFP*-*mpeg:mCherry* zebrafish larva showing brain vasculature in green and microglial cells in red. Dorsal view with the caudal tail up. ROI is delimited by a white dashed square (See Supplemental Movie 2 for precise anatomical reference). Scale bar: 50 μ m. **B)** Microglia detail of CTRL (B), 0.1 μ g/L (B1) and 1000 μ g/L (B2) glyphosate. Scale bar: 20 μ m (See Supplemental Movies 3 and 4 for single cell details). White arrows indicate activated microglia, white arrowheads indicate rod-like microglia, and white asterisk resting microglia. **C)** Number of microglial cells within the selected ROI (Kruskal-Wallis, Dunn's multiple comparisons test, $H_2=1.711$, $p=0.4252$). **D)** Quantification of microglia cells according to morphology. Asterisks indicate significant differences between CTRL and glyphosate groups (2-way ANOVA, interaction $p<0.0001$, morphology $p<0.0001$, experimental group $p=0.9639$, Dunnett's multiple comparisons test, * $p<0.05$, ** $p<0.01$, *** $p<0.001$, **** $p<0.0001$). Data refer to $n=10$ /condition.

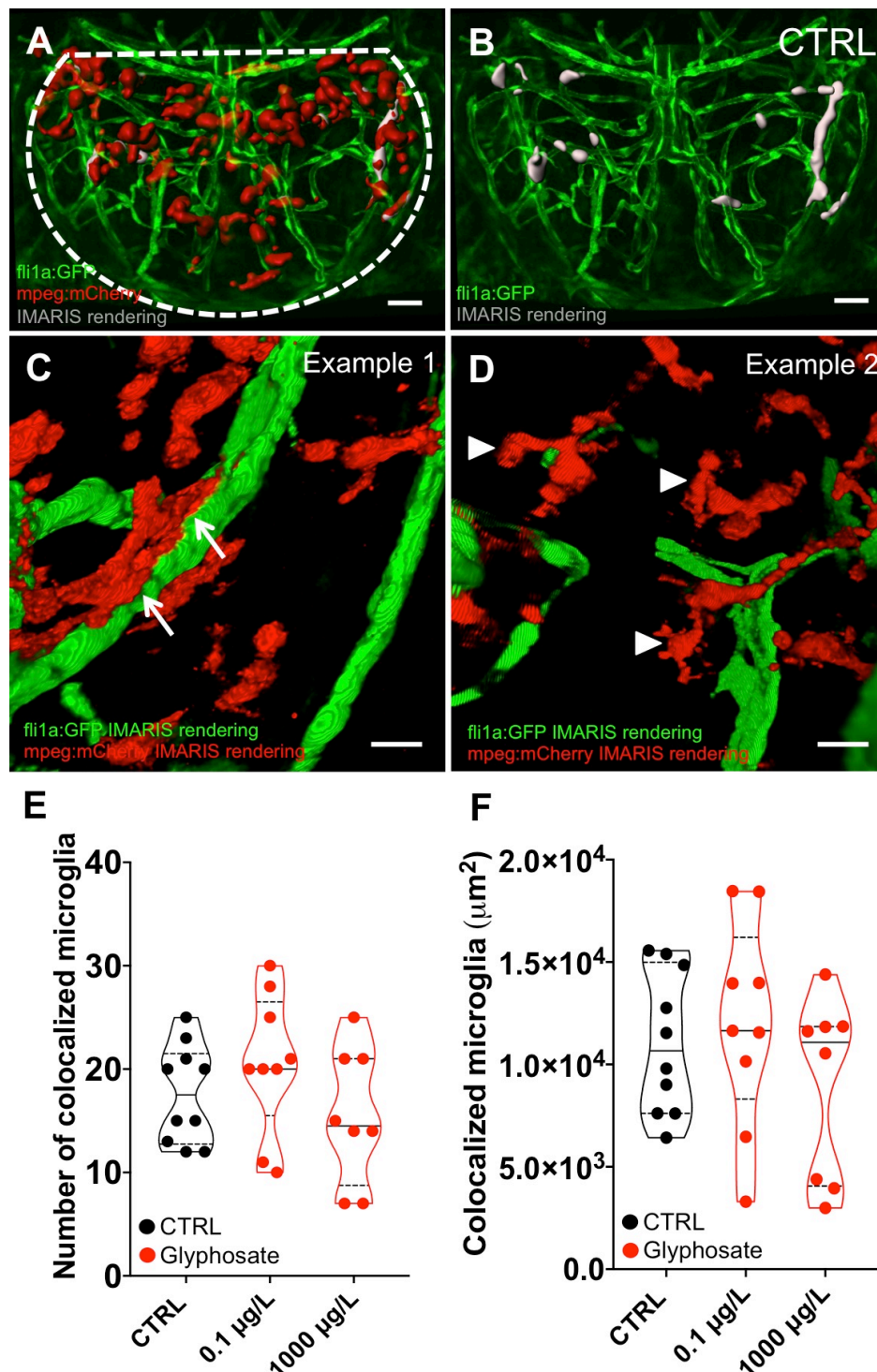


Figure 6. Patterns of cerebrovascular-microglia spatial distribution. **A)** 2-photon projected z-stack images of a *fli1a:GFP* - *mpeg:mCherry* zebrafish larvae. **B)** Example of isosurface (Imaris rendering) used for quantifications, indicating in grey the regions of microglia contacting vessels (CTRL). Scale bar: 10 μm . **C)** Example of microglia cell juxtaposed to a vessel (white arrow). **D)** Example of parenchymal microglia (arrowheads); **E)** number of co-localized or juxtaposed microglia-vessel. **F)** Area of juxtaposed microglia-vessels / μm^2 (1-way ANOVA, Dunnett's multiple comparisons test, $p < 0.05$). Data refer to $n=10/\text{condition}$.

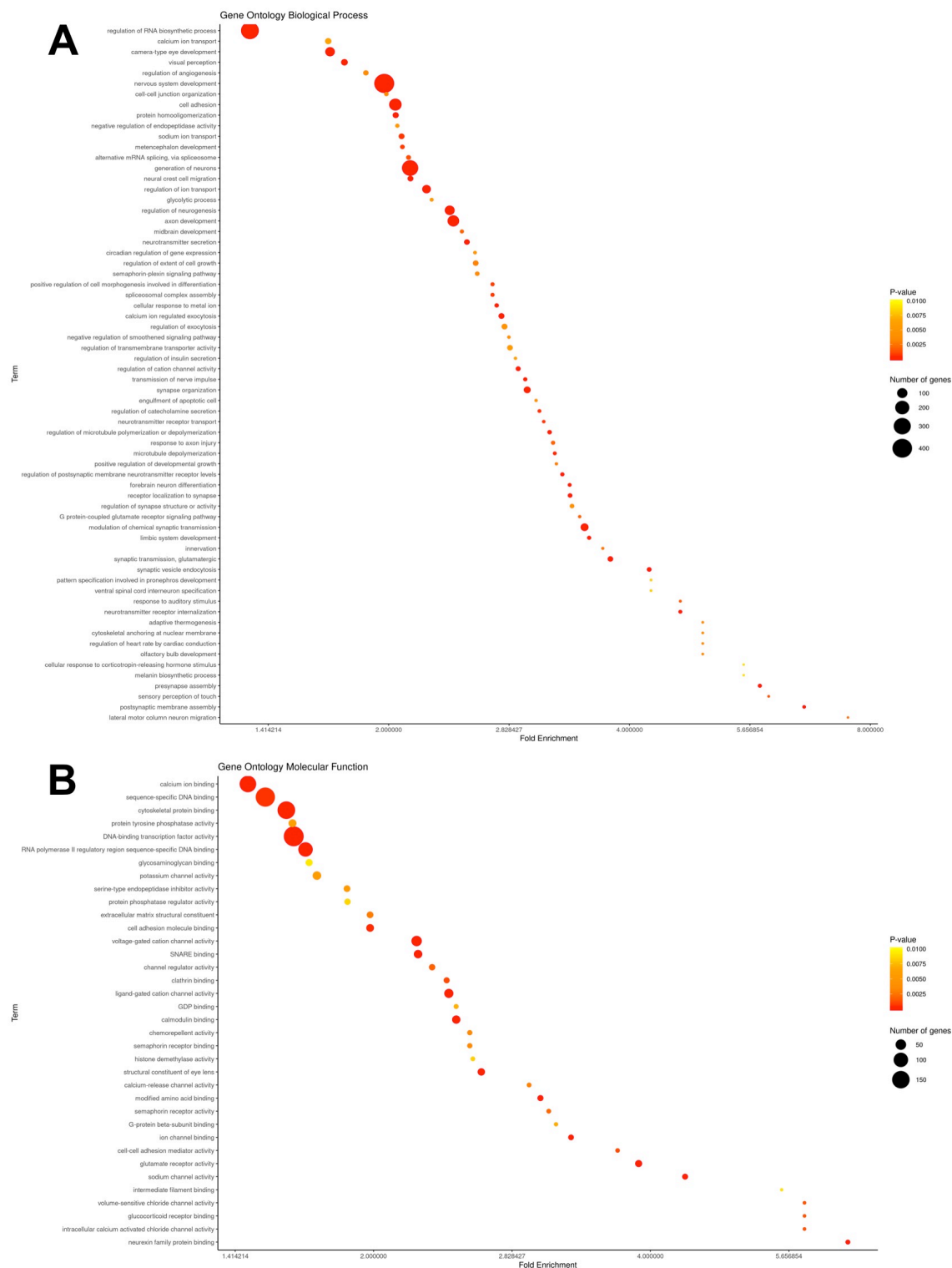


Figure 7. Transcriptome analyses revealed differentially expressed genes after glyphosate exposure. **A)** Examples of fairy lights graphs relative to 1000 µg/L glyphosate (as compared to control) for biological processes and **B)** molecular functions. Graphs relative to 0.1 µg/L glyphosate are provided in Supplemental Figure 2. Circles size represents the number of genes included in each category (listed in Y axis), color coded to represent p-values (from 0.01 yellow to 0.0025 red). The complete gene list for each category (Y axis) is provided in Supplemental Tables 4 – 6. The 10 most deregulated pathways for both categories are provided in Table 2. Data refer to n = 3 / condition and 70 larvae were pooled for each replicate.

Table 1. GO Enrichment analysis (Biological Processes and Molecular Functions) relative to 0.1 µg/L glyphosate vs. control. GO.ID: gene Ontology identifier; Term: description of the GO.ID; Annotated: number of genes on the reference; Significant: number of differentially expressed genes; Genes: 5 most deregulated genes for each pathway with the p-value. See Supplemental Table 1, 2, 3. Red: downregulated genes; green: upregulated genes.

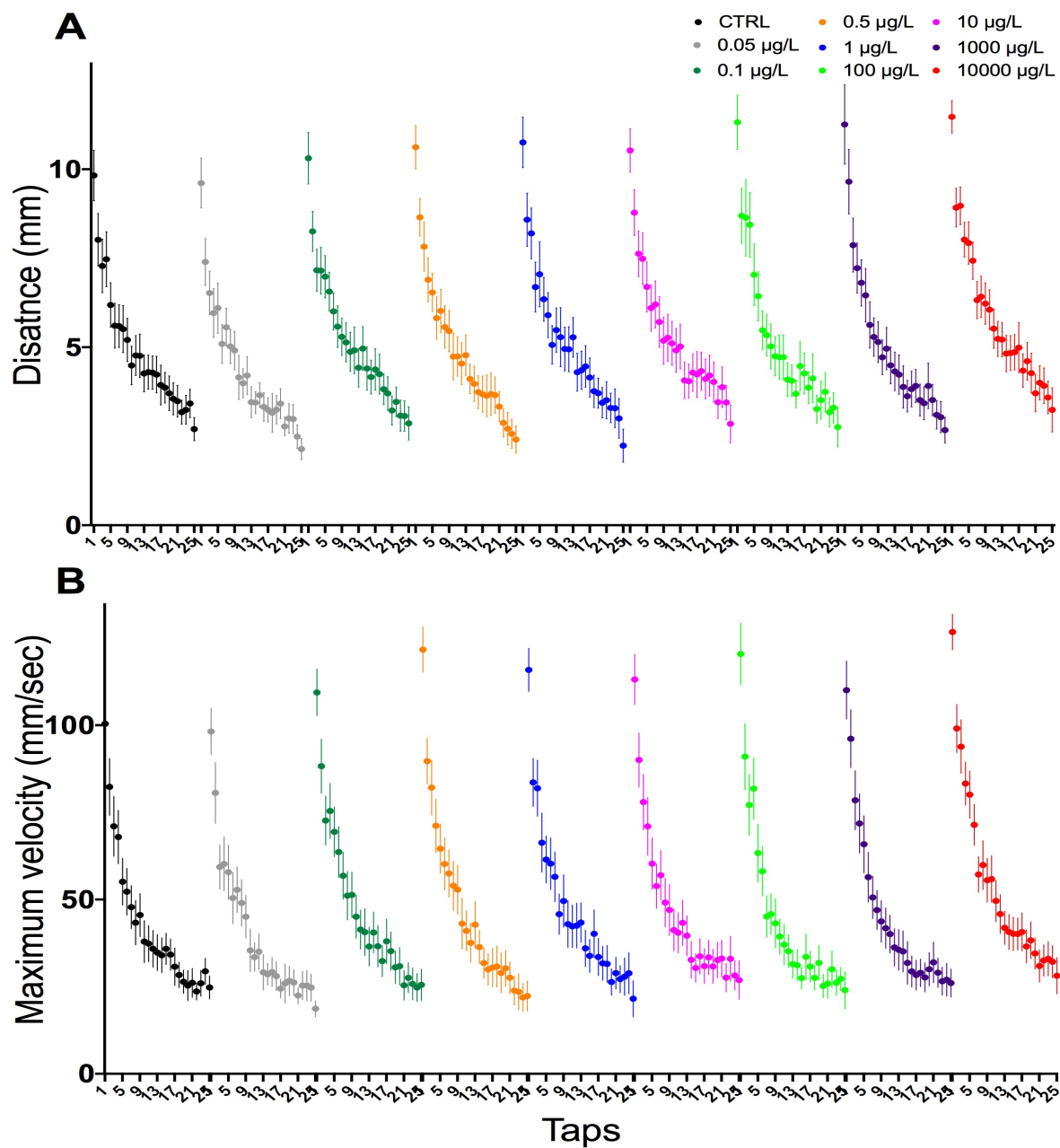
BIOLOGICAL PROCESSES				
GO.ID	Term	Annotated	Significant	Gene
GO:0006811	ion transport	1005	249	<i>snx16, slc17a6a, glra1, kcnc3b, syt2a</i>
GO:0055085	transmembrane transport	987	217	<i>slc17a6a, glra1, sv2c, kcnc3b, abcg4a</i>
GO:0031175	neuron projection development	532	129	<i>map1aa, tnc, epha4b, b3gat1a, nadl1.1</i>
GO:0007268	chemical synaptic transmission	334	120	<i>napba, slc17a6a, glra1, stx1b, sv2c</i>
GO:0098662	inorganic cation transmembrane transport	372	101	<i>kcnc3b, cacna1ab, fxyd6, kcnc3a, kcnh7</i>
GO:0048667	cell morphogenesis involved in neuron differentiation	402	95	<i>map1aa, tnc, epha4b, nadl1.1, zmp:0000001168</i>
GO:0061564	axon development	400	94	<i>map1aa, tnc, epha4b, b3gat1a, nadl1.1</i>
GO:0098609	cell-cell adhesion	305	86	<i>celsr3, pcdh2ac, tenm1, pcdh7a, pcdhb</i>
GO:0043269	regulation of ion transport	226	79	<i>snx16, kcnc3b, syt2a, cacna1ab, syt7b</i>
GO:0042391	regulation of membrane potential	148	59	<i>snx16, glra1, gabra1, kcnh7, gabrb1</i>
MOLECULAR FUNCTION				
GO.ID	Term	Annotated	Significant	Gene
GO:0046873	metal ion transmembrane transporter activity	430	148	<i>kcnc3b, slc6a19a.1, ryr2a, asic2, slc8a4a</i>
GO:0005509	Calcium ion binding	672	122	<i>syt2a, celsr3, pcdh2ac, ryr2a, pla2g12b</i>
GO:0005261	cation channel activity	325	121	<i>kcnc3b, ryr2a, asic2, cacna1ab, kcnc3a</i>
GO:0008092	cytoskeletal protein binding	693	103	<i>map1aa, apc2, map6b, myo15aa, map6a</i>
GO:0015276	ligand-gated ion channel activity	155	58	<i>glra1, asic2, gabra1, gabrb1, si:dkey-155h10.3</i>
GO:0005096	GTPase activator activity	196	34	<i>si:dkey-191m6.4, arhgap39, zmp:0000001168, sgsm1a, sgsm1b</i>
GO:0042802	identical protein binding	196	34	<i>glra1, tenm1, tenm3, si:dkey-237h12.3, plxna3</i>
GO:0022824	transmitter-gated ion channel activity	65	33	<i>glra1, gabra1, si:dkey-155h10.3, gabra3, grin2da</i>
GO:0003774	motor activity	147	28	<i>myo15aa, kif21a, myo9ab, myo16, myo9ab</i>
GO:0046906	tetrapyrrole binding	165	26	<i>cyp3c4, cyp3c3, cyp2n13, cyp2r1, cyp2aa8</i>

Table 2. GO Enrichment analysis (Biological Processes and Molecular Functions) relative to 1000 µg/L glyphosate vs. control. GO.ID: gene Ontology identifier; Term: description of the GO.ID; Annotated: number of genes on the reference; Significant: number of differentially expressed genes; Genes: 5 most deregulated genes for each pathway with the p-value. See Supplemental Table 4, 5, 6 or Figure 7 for a schematic representation. Red: downregulated genes; Green: upregulated genes.

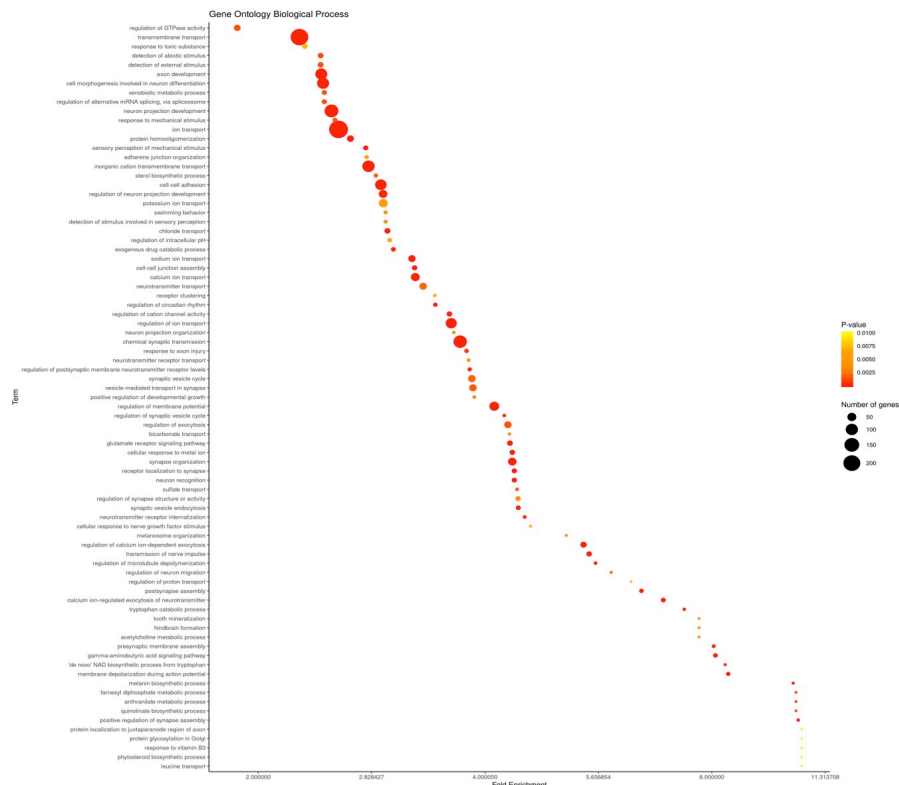
BIOLOGICAL PROCESSES				
GO.ID	Term	Annotated	Significant	Gene
GO:0007399	nervous system development	1543	411	<i>robo1, nr4a2b, plxna3, smc1a, usp28</i>
GO:2001141	regulation of RNA biosynthetic process	1796	325	<i>nr1d2a, nr4a2b, myt1b, eomesa, nr4a3</i>
GO:0048699	generation of neurons	934	268	<i>robo1, nr4a2b, plxna3, stmn2b, tor1l2</i>
GO:0007155	cell adhesion	549	151	<i>plxna3, cdh7, cel.1, tor1l2, robo4</i>
GO:0061564	axon development	400	130	<i>robo1, plxna3, thsd7aa, robo4, ephb3a</i>
GO:0050767	regulation of neurogenesis	283	91	<i>plxna3, si:dkey-114c15, zic5, robo2, daam2</i>
GO:0043010	camera-type eye development	373	85	<i>foxg1a, crygm2d10, sox4b, sox4a, fgf19</i>
GO:0043269	regulation of ion transport	226	68	<i>syt12, snc1ba, si:dkey-56f14.4, cacng5a, cacnb1</i>
GO:0050804	modulation of chemical synaptic transmission	116	55	<i>syt12, cel.1, atcaya, grm2b, nlgn4a</i>
GO:0050808	synapse organization	102	41	<i>cel.1, nbeaa, pick1, nlgn4a, tnc</i>
MOLECULAR FUNCTION				
GO.ID	Term	Annotated	Significant	Gene
GO:0003700	DNA-binding transcription factor activity	883	196	<i>nr1d2a, nr4a2b, myt1b, eomesa, nr4a3</i>
GO:0043565	sequence-specific DNA binding	890	184	<i>nr1d2a, nr4a2b, myt1b, si:ch211-69l10.4, eomesa</i>
GO:0008092	cytoskeletal protein binding	693	151	<i>myhb, stmn2b, cdh7, tor1l2, lmod2b</i>
GO:0005509	calcium ion binding	672	133	<i>si:ch211-202f3.3, nell2a, cdh7, syt12, edil3a</i>
GO:0000977	RNA polymerase II regulatory region sequence-specific DNA binding	433	99	<i>nr4a2b, myt1b, eomesa, nr4a3, yy1b</i>
GO:0022843	voltage-gated cation channel activity	159	48	<i>cacng5a, cacnb1, kcnj13, cacna1sb, kcnj3b</i>
GO:0099094	ligand-gated cation channel activity	110	36	<i>ryr3, asic1b, asic1a, kcnj13, kcnj3b, jph1b</i>
GO:0005267	potassium channel activity	136	32	<i>kcnj13, kcnj3b, kcne4, kcnc1a, kcnj11l</i>
GO:0000149	SNARE binding	99	30	<i>syt12, si:dkey-196h17.9, sya, stx12l, cplx2</i>
GO:0005516	calmodulin binding	87	29	<i>marcksa, marcksb, marcksl1a, camk4, cnn1a</i>

Table 3. GO Enrichment analysis (Biological Processes and Molecular Functions) relative to 0.1 µg/L vs. 1000 µg/L glyphosate. GO.ID: gene Ontology identifier; Term: description of the GO.ID; Annotated: number of genes on the reference; Significant: number of differentially expressed genes; Genes: 5 most deregulated genes for each pathway with the p-value. See Supplemental Table 7, 8, 9. See fairy light graphs in Supplemental Figure 3. Red: downregulated genes; green: upregulated genes.

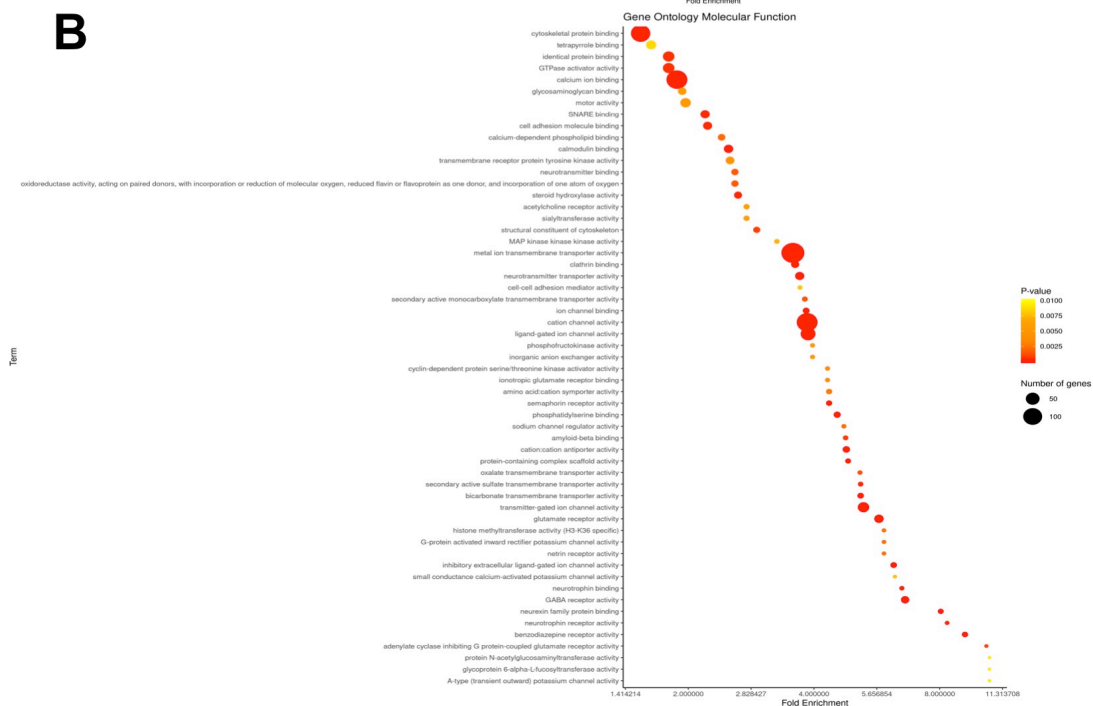
BIOLOGICAL PROCESSES				
GO.ID	Term	Annotated	Significant	Gene
GO:0055114	oxidation-reduction process	735	122	<i>rpe65a</i> , <i>prdx1</i> , <i>zgc:163022</i> , <i>gyg2</i> , <i>miox</i>
GO:0006412	translation	432	82	<i>eif4a1a</i> , <i>gfm1</i> , <i>drg1</i> , <i>zgc:162730</i> , <i>eef1a1l2</i>
GO:0042254	ribosome biogenesis	209	55	<i>abt1</i> , <i>urb2</i> , <i>noc4l</i> , <i>dkc1</i> , <i>mrto4</i>
GO:0006260	DNA replication	128	39	<i>mcm2</i> , <i>mcm5</i> , <i>mcm3</i> , <i>mcm6</i> , <i>msh6</i>
GO:0007601	visual perception	160	37	<i>rpe65a</i> , <i>per1b</i> , <i>guca1e</i> , <i>opn1mw2</i> , <i>rgra</i>
GO:0006457	protein folding	127	33	<i>hsp90aa1.1</i> , <i>hspd1</i> , <i>ptges3b</i> , <i>dnajb11</i> , <i>pdia2</i>
GO:0002088	lens development in camera-type eye	93	24	<i>unc45b</i> , <i>crygm2d10</i> , <i>crygm2c</i> , <i>crygm2d6</i> , <i>crygm2d18</i>
GO:0042737	drug catabolic process	107	21	<i>prdx1</i> , <i>chia.3</i> , <i>chia.6</i> , <i>cat</i> , <i>hpda</i>
GO:0071466	cellular response to xenobiotic stimulus	90	20	<i>sult1st2</i> , <i>ca2</i> , <i>sult1st1</i> , <i>pck2</i> , <i>sult1st3</i>
GO:0016126	sterol biosynthetic process	36	19	<i>apoa4a</i> , <i>cyb5r2</i> , <i>zgc:162608</i> , <i>fdft1</i> , <i>sc5d</i>
MOLECULAR FUNCTION				
GO.ID	Term	Annotated	Significant	Gene
GO:0030554	adenyl nucleotide binding	1686	215	<i>gluc</i> , <i>acss2l</i> , <i>hsp90aa1.1</i> , <i>si:dkey-71l4.4</i> , <i>hspa4a</i>
GO:0048037	cofactor binding	481	78	<i>aifm4</i> , <i>mtr</i> , <i>porb</i> , <i>cyb5r2</i> , <i>mthfr</i>
GO:0003735	structural constituent of ribosome	157	34	<i>faub</i> , <i>mrpl12</i> , <i>mrps31</i> , <i>rpl7l1</i> , <i>mrpl43</i>
GO:0016853	isomerase activity	134	30	<i>rpe65a</i> , <i>pdia2</i> , <i>pmm2</i> , <i>ebp</i> , <i>dkc1</i>
GO:0046906	tetrapyrrole binding	165	28	<i>mtr</i> , <i>cyb5b</i> , <i>cat</i> , <i>zgc:136333</i> , <i>cyp3c4</i>
GO:0030414	peptidase inhibitor activity	167	27	<i>muc5.1</i> , <i>lxn</i> , <i>serpina1l</i> , <i>si:busm1-57f23.1</i> , <i>serpine2</i>
GO:0051082	unfolded protein binding	91	26	<i>hsp90aa1.1</i> , <i>uggt1</i> , <i>dnajb11</i> , <i>calr3b</i> , <i>hsp70.3</i>
GO:0005212	structural constituent of eye lens	62	21	<i>crygm2d10</i> , <i>crygm2c</i> , <i>crygm2d6</i> , <i>crygm2d18</i> , <i>crygm2d21</i>
GO:0003697	single-stranded DNA binding	60	18	<i>mcm2</i> , <i>mcm5</i> , <i>mcm3</i> , <i>mcm6</i> , <i>ssbp1</i>
GO:0016765	transferase activity, transferring alkyl or aryl (other than methyl) groups	57	17	<i>fdps</i> , <i>fdft1</i> , <i>mat2ab</i> , <i>srm</i> , <i>hmbsb</i>



A

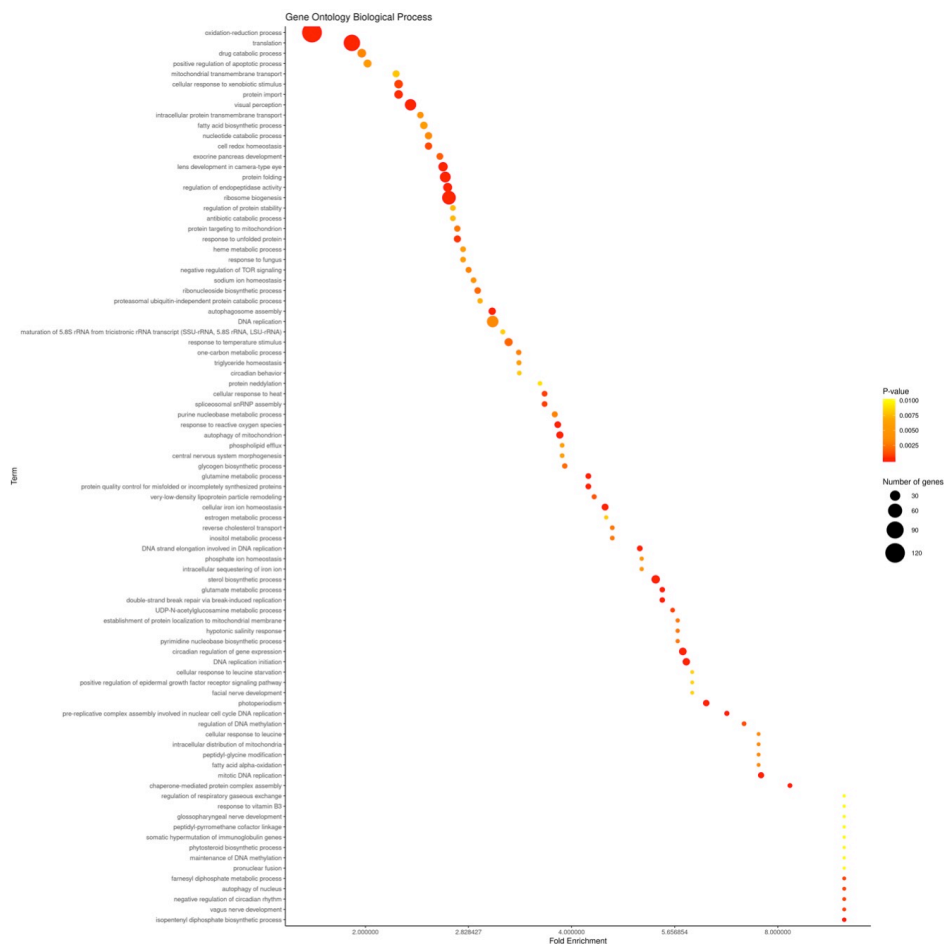


B

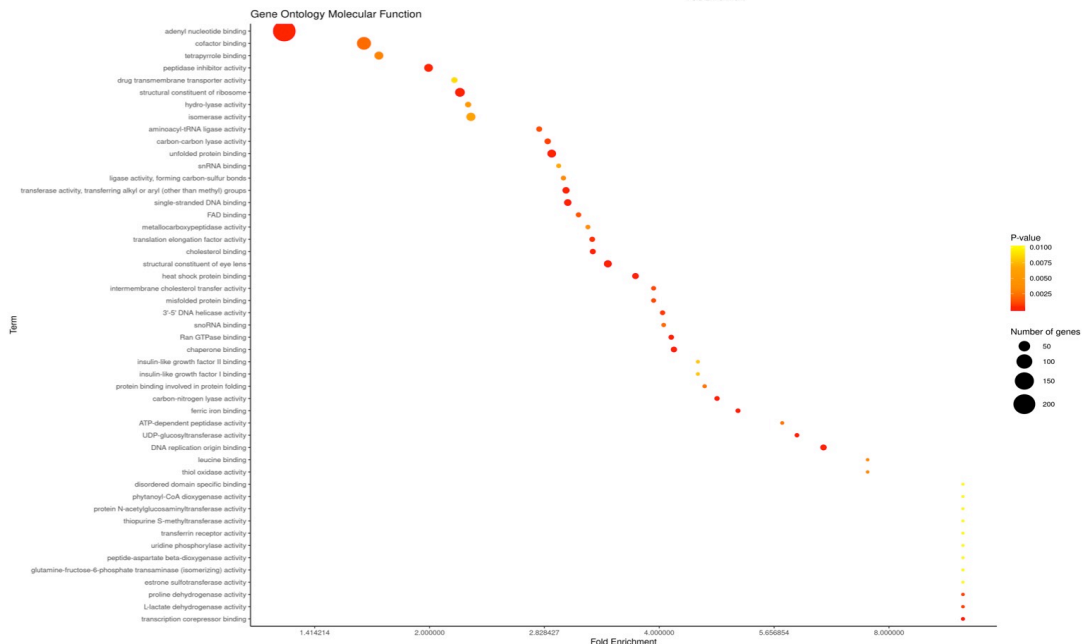


Supplemental Figure 2. Transcriptome analyses revealed differentially expressed genes after glyphosate exposure. A) Examples of fairy lights graphs relative to 0.1 µg/L glyphosate (as compared to control) for biological processes and B) molecular functions. Circles size represents the number of genes included in each category (listed in Y axis), color coded to represent p-values (from 0.01 yellow to 0.0025 red). The complete gene list for each category (Y axis) is provided in Supplemental Tables 1 – 3. The 10 most deregulated pathways for both categories are provided in Table 1. Data refer to n = 3 / condition. N = 70 larvae were pooled per replicate.

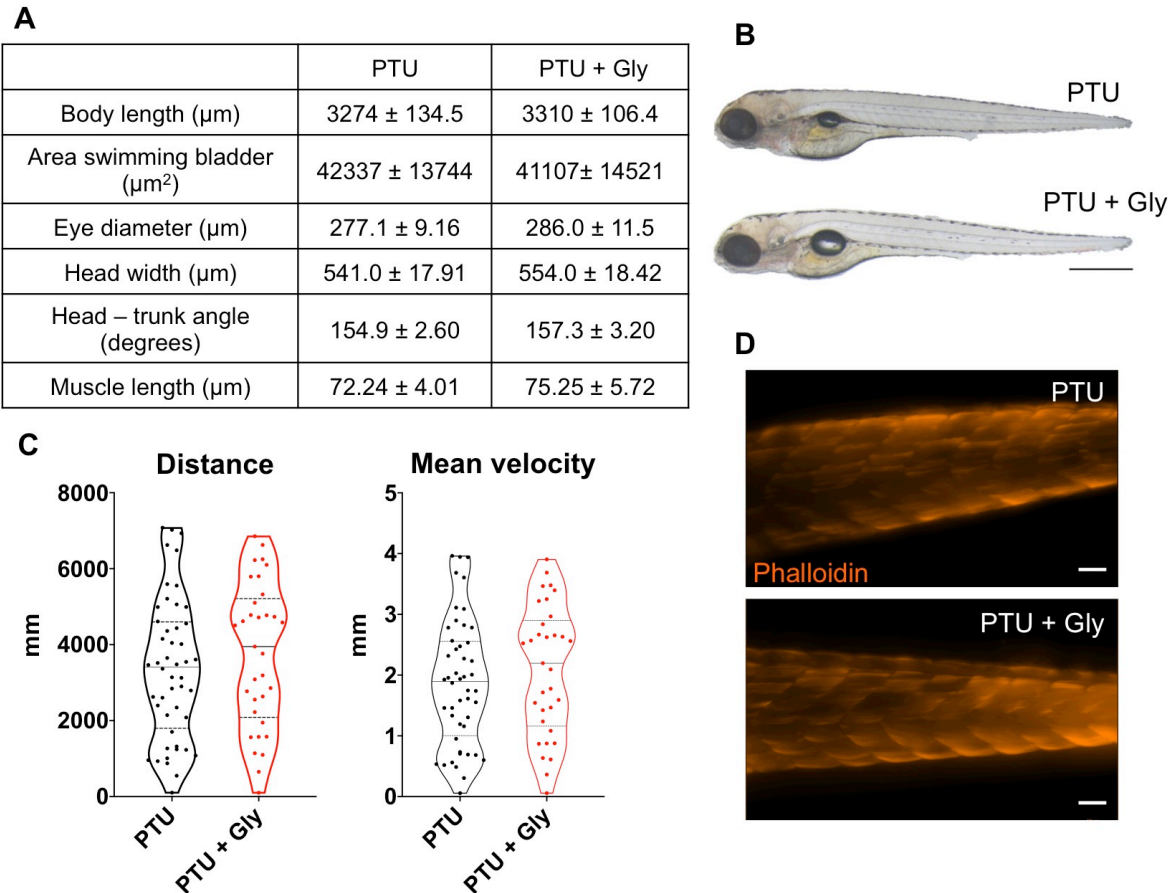
A



B



Supplemental Figure 3. Transcriptome analyses revealed differentially expressed genes after glyphosate exposure. **A)** Examples of fairy lights graphs relative 0.1 µg/L vs. 1000 µg/L glyphosate for biological processes and **B)** molecular functions. Circles size represents the number of genes included in each category (listed in Y axis), color coded to represent p-values (from 0.01 yellow to 0.0025 red). The complete gene list for each category (Y axis) is provided in Supplemental Tables 7 – 9. The 10 most deregulated pathways for both categories are provided in Table 3. Data refer to n = 3 / condition. N= 70 larvae were pooled per replicate.



Supplemental Figure 4. A) Morphological parameters: Total body length (μm), swimming bladder (μm²), eye diameter (μm) and trunk-head angle (degrees), muscle fibre length (μm) of zebrafish larvae at 120 hpf (t test, p<0.05). Data reported as means ± SD. Experiments conducted in duplicate (n = 10/group; phalloidin PTU n = 3, PTU+Gly n = 7). **B)** Examples for morphological assessments. Scale bar: 500 μm. **C)** Locomotor test in zebrafish larvae at 120 hpf: Distance (mm) and mean velocity (mm/sec), data reported as means ± SD (t test, p<0.05), experiments conducted in duplicate (n = 48/group). **D)** Examples of lateral views of trunk somites in zebrafish larvae stained using phalloidin of PTU and PTU + Gly.

Supplemental Movie 1: details of fli1a:GFP cerebrovasculature.
Supplemental Movie 2: fli1a:GFP delimited ROI for mpeg:mCherry microglial quantification.
Supplemental Movies 3 and 4: details of resting and activated mpeg:mCherry microglial cells.

Supplemental Table RNAseq raw data
Supplemental Tables 1 – 3: Statistical analysis of enriched GO processes for 0.1 μg/L glyphosate exposure as compared to control: biological processes, molecular functions and cellular components, respectively.
Supplemental Tables 4 – 6: Statistical analysis of enriched GO processes for 1000 μg/L glyphosate exposure as compared to control: biological processes, molecular functions and cellular components, respectively.

1080 **Supplemental Tables 7 – 9:** Statistical analysis of enriched GO processes for the
1081 comparison 0.1 µg/L vs. 1000 µg/L glyphosate exposure: biological processes,
1082 molecular functions and cellular components, respectively.